

**THE EVALUATION OF THE MECHANICAL STRENGTH OF EPOXY-BASED
RESIN AS A PLUGGING MATERIAL, AND THE DEVELOPMENT OF A
NOVEL PLUG AND ABANDON TECHNIQUE USING VITRIFIED SOLID
EPOXY-BASED RESIN BEADS**

A Thesis

by

AHMED RAMI ABUELAISH

Submitted to the Office of Graduate Studies of
Texas A&M University
in partial fulfillment of the requirements for the degree of
MASTER OF SCIENCE

May 2012

Major Subject: Petroleum Engineering

The Evaluation of the Mechanical Strength of Epoxy-Based Resin as a Plugging
Material, and the Development of a Novel Plug and Abandon Technique Using Vitrified

Solid Epoxy-Based Resin Beads

Copyright 2012 Ahmed Rami Abuelaish

**THE EVALUATION OF THE MECHANICAL STRENGTH OF EPOXY-BASED
RESIN AS A PLUGGING MATERIAL, AND THE DEVELOPMENT OF A
NOVEL PLUG AND ABANDON TECHNIQUE USING VITRIFIED SOLID
EPOXY-BASED RESIN BEADS**

A Thesis

by

AHMED RAMI ABUELAISH

Submitted to the Office of Graduate Studies of
Texas A&M University
in partial fulfillment of the requirements for the degree of

MASTER OF SCIENCE

Approved by:

Co-Chairs of Committee, Hisham Nasr-El-Din
Jerome Schubert
Committee Member, Mahmoud El-Halwagi
Head of Department, Stephen Holditch

May 2012

Major Subject: Petroleum Engineering

ABSTRACT

The Evaluation of the Mechanical Strength of Epoxy-Based Resin as a Plugging Material, and the Development of a Novel Plug and Abandon Technique Using Vitrified Solid Epoxy-Based Resin Beads. (May 2012)

Ahmed Rami Abuellaish, B.S., Texas A&M University

Co-Chairs of Advisory Committee: Dr. Hisham Nasr-El-Din
Dr. Jerome Schubert

Over the past several years, some of the platforms in the Gulf of Mexico have been damaged completely, such that conventional P&A operations may not be possible. In these cases, plugging fluid needs to be pumped through an intervention well and dropped several thousand feet in water to settle above a packer and seal the well.

The current P&A material of choice is cement, but cement is miscible in water, which dilutes and contaminates the cement. Therefore, alternate plugging materials need to be used for these operations. This paper discusses the development of a cost-effective Epoxy P&A method and the challenges of using Epoxy. First, the impact of seawater, oil, and pipe dope on the curing process remains unknown. Secondly, the yield strength of Epoxy with and without the contaminating chemicals must be equal to or better than cement. Finally, previous tests have shown significant losses of Epoxy to the walls of the wellbore during the 7,000-ft drop.

High temperature curing and compression tests were performed on contaminated epoxy samples to determine the effectiveness of the epoxy plug. To reduce material losses, an improved method for introducing the epoxy into the target zone was developed. This method takes advantage of a narrow window in the cure process where the curing process can be suspended by quenching the partially cured liquid epoxy in water at room temperature, thereby changing the liquid epoxy into solid beads. The beads can then be pumped into the wellbore, where they liquefy at wellbore temperature, 200°F, then cure into a solid plug.

Seawater was found to accelerate the cure time, while all contaminants tested reduced the fracture strength by more than 25% compared to pure resin. The yield strengths of contaminant mixtures, however, remained relatively constant, with the greatest drop being only 11%. The use of solid epoxy beads was found to have a compressive strength 50% greater than Portland cements I&II. In addition, the application mentioned herein eliminates the need to prepare the plug material on site. These advantages greatly contribute to reducing the costs of an epoxy P&A operation, to potentially being USD 0.7 million cheaper than a Portland cement operation.

ACKNOWLEDGEMENTS

I would like to thank my committee chair, Dr. Nasr-El-Din, and my committee members, Dr. Schubert, and Dr. El-Halwagi, for their guidance and support throughout the course of this research.

Thanks also go to my friends and colleagues and the department faculty and staff for making my time at Texas A&M University a great experience. I also want to extend my gratitude to the BOEMRE for funding this research, Professional Fluids Systems for providing me with all the resin I needed for the experiments, and Best-o-life for providing me with all the pipe dope material I needed.

Finally, thanks to my mother and father for their encouragement and support.

NOMENCLATURE

bbl/bbls	Barrel/barrels
BOEMRE	The Bureau of Ocean Energy Management, Regulation & Enforcement
deg	Degrees
ft	Foot/feet
g	Gram
gal	Gallons
GOM	Gulf of Mexico
ID	Inner diameter
in	Inch
lb/lbs	Pound/pounds
min	Minutes
mL	Milliliters
MMS	Mineral Management Services
O&G	Oil and Gas
OD	Outer diameter
P&A	Plug and Abandon
PFS	Professional Fluid Services
ppg	Pounds per gallon
PVC	Polyvinyl chloride

sec/secs	Second/seconds
TETA	Tri-ethylene-tetra-amine
TTT	Time-temperature-transformation diagram
TVD	True Vertical Depth
TVDSS	True Vertical Depth Subsea
WOC	Wait on Cement
WGSO	Water/Gas Shutoff
vs.	Versus

TABLE OF CONTENTS

	Page
ABSTRACT.....	iii
ACKNOWLEDGEMENTS	v
NOMENCLATURE	vi
TABLE OF CONTENTS	viii
LIST OF FIGURES	x
LIST OF TABLES	xv
CHAPTER I INTRODUCTION	1
CHAPTER II LITERATURE REVIEW.....	6
CHAPTER III PRIMARY OBJECTIVES.....	12
CHAPTER IV MECHANICAL STRENGTH TESTS.....	14
Background.....	14
Epoxy-Based Resin.....	14
Pipe Dope	15
Properties of Wells in the Gulf of Mexico	16
Mechanical Strength	18
Failure Modes.....	21
Objectives	22
Procedure.....	23
Results and Discussion.....	27
Pure Epoxy-Based Resin.....	27
Seawater Brine.....	29
Pipe Dope	33
Sour Oil	46
Fracture Strength	49
CHAPTER V EVALUATING THE EFFECT OF CONTAMINANTS ON THE CURE PROCESS OF EPOXY RESIN.....	52
Objective.....	52
Procedure.....	52
Level of Gelation	54

	Page
Results and Discussion.....	55
Pure Epoxy-Based Resin.....	55
Seawater Brine.....	56
Sour Oil.....	59
Pipe Dope.....	61
CHAPTER VI EVALUATING THE USE OF SOLID EPOXY BEADS AS A PLACEMENT METHOD	63
Background.....	63
Vitrification and Gelation	63
Portland Cement	65
Objectives	66
Procedure.....	66
Results and Discussion.....	72
Cost Analysis.....	77
CHAPTER VII CONCLUSIONS.....	79
REFERENCES	81
VITA.....	84

LIST OF FIGURES

	Page
Fig. 1—Using an offset well to gain access to the wellbore	3
Fig. 2—The structure of a phenol-formaldehyde (Peng and Riedl 1995)	7
Fig. 3—Synthesis of a Bisphenol A based epoxy resin (Irfan 1998)	7
Fig. 4—Placing the epoxy resin in the thief zone and allowing it to cure, then milling out the hardened solid to the same inner diameter of the casing (Ng 1995)	8
Fig. 5—Epoxy breaking down into smaller droplets and spreading in a column of water (El-Mallawany 2011).....	11
Fig. 6—The approximate temperature increase per 1,000 ft True Vertical Depth Subsea based on a 0.8 °F/100ft and 1.9 °F/100ft rate (data from API 1999).....	17
Fig. 7—Applied axial compression force P on the normal cross-sectional area A of a cylindrical specimen.....	19
Fig. 8—Stress-Strain curve for a brittle material (after Case et al. 1999)	20
Fig. 9—Stress-Strain curve for a ductile material (after Case et al. 1999)	21
Fig. 10—Failure showing a fracture in a diagonal plane due to compressive loading on a specimen of a brittle material	22
Fig. 11—Barrel-like failure due to compression on a specimen of ductile material	22
Fig. 12—The Instron 4206 used for compression tests with a load limit up to 30,000 psi	26
Fig. 13—The control panel for the Instron 4206.....	27
Fig. 14—The stress-strain curve from 6 experiment runs for pure epoxy-based resin, tested under compression until failure.....	28
Fig. 15—A specimen of pure epoxy-based resin before and after the compression test	29

	Page
Fig. 16—The separation of resin and seawater brine is apparent due to the fluids being immiscible	29
Fig. 17—An emulsion of resin droplets in seawater brine during and after mixing for one hour prior to curing.....	30
Fig. 18—Epoxy and seawater brine mixture after being mixed for an hour then settling for approximately 15 minutes in a 200 °F oven	31
Fig. 19—The stress-strain curve from different experiment runs for epoxy-based resin with seawater brine, tested under compression until failure	32
Fig. 20—A specimen of fully cured resin mixed with seawater brine before and after the compression test	32
Fig. 21—ZN18 thread compound.....	34
Fig. 22—The fully cured sample of resin mixed with ZN18 pipe dope	34
Fig. 23—The stress-strain curve from different experiment runs for epoxy-based resin with ZN18 pipe dope, tested under compression until failure.....	35
Fig. 24—A specimen of fully cured resin mixed with ZN18 pipe dope before and after the compression test	35
Fig. 25—API-Modified pipe dope compound	36
Fig. 26—The fully cured sample of resin mixed with API-Modified pipe dope	36
Fig. 27—The stress-strain curve from different experiment runs for epoxy-based resin with API-Modified pipe dope, tested under compression until failure....	37
Fig. 28—A specimen of fully cured resin mixed with API-Modified pipe dope before and after the compression test	38
Fig. 29—2000 pipe dope compound.....	38
Fig. 30—The fully cured sample of resin mixed with 2000 pipe dope	39
Fig. 31—The stress-strain curve from different experiment runs for epoxy-based resin with 2000 pipe dope, tested under compression until failure	40

Fig. 32—A specimen of fully cured resin mixed with 2000 pipe dope before and after the compression test	40
Fig. 33—OCTG pipe dope compound.....	41
Fig. 34—The fully cured sample of resin mixed with OCTG pipe dope	41
Fig. 35—The stress-strain curve from different experiment runs for epoxy-based resin with OCTG pipe dope, tested under compression until failure	42
Fig. 36—A specimen of fully cured resin mixed with OCTG pipe dope before and after the compression test	42
Fig. 37—Metal-free pipe dope compound	43
Fig. 38—The fully cured sample of resin mixed with Metal-free pipe dope.....	43
Fig. 39—The stress-strain curve from different experiment runs for epoxy-based resin with Metal-free pipe dope, tested under compression until failure	44
Fig. 40—A specimen of fully cured resin mixed with Metal-free pipe dope before and after the compression test.....	44
Fig. 41—4010NM pipe dope compound	45
Fig. 42—The fully cured sample of resin mixed with 4010NM pipe dope	45
Fig. 43—The stress-strain curve from different experiment runs for epoxy-based resin with 4010NM pipe dope, tested under compression until failure.....	46
Fig. 44—A specimen of fully cured resin mixed with 4010NM pipe dope before and after the compression test.....	46
Fig. 45—The fully cured sample of resin mixed with sour oil	47
Fig. 46—The stress-strain curve from different experiment runs for epoxy-based resin with Sour Oil, tested under compression until failure	48
Fig. 47—A specimen of fully cured resin mixed with oil before and after the compression test.....	48
Fig. 48—The average fracture strengths of samples in comparison to their average yield strengths	50

	Page
Fig. 49—The 3mm metal rod used in the qualitative level of gelation test	54
Fig. 50—Thick, clear, orange colored, viscous epoxy resin	55
Fig. 51—The curing trend for pure epoxy-based resin which shows a decrease in the level of Gelation during the first hour, then a gradual increase until full cure at 6 hours	56
Fig. 52—The curing trend for epoxy-based resin in the presence of seawater brine at 10, 20, 30, 40, and 50 wt % seawater	57
Fig. 53— The curing trend for epoxy-based resin in the presence of 50 wt % of 5 brines at 2 different concentrations	59
Fig. 54—The curing trend for epoxy-based resin in the presence of sour oil at 10, 20, 30, 40, and 50 wt % sour oil.....	60
Fig. 55—The difference in color due to the phase change of resin mixed with sour-oil caused by the change in temperature from 200 °F to room temperature.....	60
Fig. 56—The curing trend for epoxy-based resin in the presence of the 6 types of Best-o-life pipe dopes: OCTG, 2000, API modified, 4010NM, ZN18, and Metal Free	62
Fig. 57—An isothermal time-temperature-transformation (TTT) diagram showing the onset of gelation, vitrification, and full cure for a thermosetting epoxy (after Gillham 1985)	64
Fig. 58—The 1-hour, 2-hour, 3-hour, and 4-hour samples of Batch B repositioned and kept in the 200°F oven	72
Fig. 59—The 5-hour samples of Batch B repositioned and kept in the 200°F oven.....	73
Fig. 60—The 6-hour, 7-hour, and 8-hour samples of Batch B repositioned and kept in the 200°F oven	73
Fig. 61—The trends of Batch A and Batch B samples showing the effect of temperature on gel strength.....	74
Fig. 62—Vitrified resin droplets that were formed by quenching droplets of resin in 39°F water 3.5 hours into the cure process.....	75

	Page
Fig. 63—A specimen of fully-cured reconstituted epoxy-resin beads before and after the compression test	76
Fig. 64—The stress-strain curve for reconstituted epoxy resin beads tested under compression until failure	77

LIST OF TABLES

	Page
Table 1—Epoxy fall rate in 30 ft of water (after El-Mallawany 2011)	10
Table 2—Mix ratios for Ultra Seal-R	15
Table 3—6 types of "Bestolife" pipe dope.....	16
Table 4—Composition of seawater	17
Table 5—Mix ratios of contaminants in resin.....	24
Table 6—Correction factor(ASTM 1999a).....	25
Table 7—Average yield strength.....	49
Table 8—Average fracture stress	51
Table 9—Composition of 4.00 gram samples.....	53
Table 10—The level of gelation	55
Table 11—Composition and concentrations of 5 brines.....	58
Table 12—Portland cement compressive strengths(data from ASTM C150/C150m)	65
Table 13—Gel strength code (Sydansk 1989)	68
Table 14—Cost comparison for P&A.....	78

CHAPTER I

INTRODUCTION

There are currently approximately 80 producing offshore rigs in the Gulf of Mexico, each with one or more drilled wells, all of which will eventually need to be plugged either temporarily or permanently once they are no longer needed. One major factor for abandoning a well is weather conditions, especially with the turbulent hurricane weather that's common in the Gulf of Mexico. Over the past several years the Bureau of Ocean Energy Management, Regulations and Enforcement (BOEMRE) reported 9 jack-up rigs and 19 moored rigs were either toppled or torn from their mooring systems by hurricanes Ivan, Katrina, and Rita. 61 platforms were destroyed as a result of hurricanes Gustav and Ike in 2008, totaling 180 destroyed and 178 damaged offshore oil and gas producing platforms between 2004 and 2008 (BOEMRE 2011). As a result of this damage, many wells can no longer produce oil and gas safely, and/or have become an environmental hazard, requiring them to be plugged and abandoned.

Standard procedures in the oil and gas industry involve using Portland cement (ASTM types I and II, or API Classes A, C, G, or H) as the plugging material. Plugs are typically placed across perforations, across certain intervals to isolate critical zones, or in the wellbore and annulus to plug and isolate the well from the surface (Kelm and Faul 1999). These procedures typically involve using a workover rig and placing the cement

This thesis follows the style of *SPE Journal*.

through tubing, drillpipe, or coil tubing at the target zone (Barclay et al. 2004; Chong et al. 2000; Tettero et al. 2004). These cement plug systems may or may not be balanced between the inside and outside volumes of the pipe which may cause the plug to contaminate and dilute, due to contact with wellbore fluids (Calvert and Smith 1994). Contaminated and diluted cement often requires the plug to be redone.

Some of the hurricane damaged platforms may have been toppled completely and destroyed, their riser damaged, or well equipment and casing damaged due to mudflow at the seabed (BOEMRE 2011). Some of these wells may still be plugged by conventional methods, but for most wells, access through the wellhead may be blocked. In this case, an offset well needs to be drilled to access the wellbore, and plugging material be allowed to drop down the well to settle on top of a packer, as displayed in **Fig. 1**. While cement is significantly cheaper than other plugging materials such as epoxy resin, it is miscible, and dilutes, in seawater and brines used as packing fluids in the Gulf of Mexico, causing it to lose its mechanical strength. To successfully place the cement plug at the target zone would require the offset well to be drilled to the target zone and cement placed using conventional methods. At a target zone depth of 7,000 ft, the time and cost of such an operation may be substantial and would cancel the competitive price advantage of cement over alternative plugging fluids.

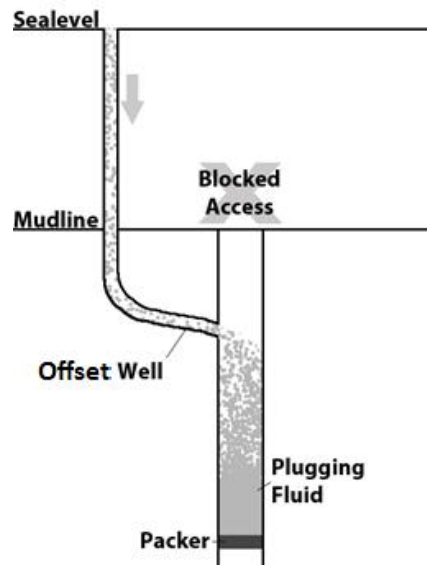


Fig. 1—Using an offset well to gain access to the wellbore

During the drop in the wellbore, the plugging fluid will be in contact with any fluid or solids that are present in the well; as a result, contamination may occur. Many studies have been conducted to identify the quantity and type of contaminants in well tubulars (Holub et al. 1974; Maly 1976; McLeod Jr. 1984; McLeod Jr. et al. 1983). It was found that one of the most prominent contaminants in production tubing or an annulus is pipe dope in addition to hydrocarbons, sand, and debris (Gougler Jr. et al. 1985; Loewen et al. 1990; Nasr-El-Din et al. 2002). If the contaminants have a deteriorating effect on the curing time of epoxy resin, it may affect the plugging effectiveness of the fluid. The contaminants may reduce the maximum compressive strength or yield strength of the plug causing the onset of crack propagation leading to a leaking plug. There is a need to study the effect of contaminants on epoxy resin, whether

curing in the presence of contaminants, or mixing with contaminants during the drop then curing to determine the applicability of these fluids.

This thesis is part of a research effort funded by the MMS (now known as BOEMRE) which aims to investigate the applicability of epoxy-based resins or other non-cement materials as plugging fluids for hurricane damaged wells in the Gulf of Mexico, as mentioned herein. The materials in question have only been used in limited permanent plug applications, and the applicability of the materials has not been sufficiently studied. The MMS aims to develop on the following points:

1. Comparing epoxy-based materials against cement abandonments and other potential plugging materials
2. Determining whether epoxy material can effectively drop 7,000 ft through a casing annuli and accumulate on top of the packer
3. Determining how long material takes to travel to the bottom of casing annuli and cure
4. Determining how material performs over time
5. Determining how weighting of this material with BaSO_4 affects the compressive and bond strength of the material
6. Determining whether there are other weighting materials which may perform better than BaSO_4
7. Ranking various resin and hardener chemical systems for best performance in the field

8. Evaluating the effects of various liquids such as calcium chloride, sea water, and formation hydrocarbons on the resin chemical systems

The research done for this thesis covers points 1 and 8 above. In addition, it addresses concerns raised by El-Mallawany regarding point 2. The work done focuses on the cure process of epoxy-based resins during the settling and curing of the plugging fluid. This thesis covers the effect of wellbore chemicals on the cure process of epoxy during the fall, where the fluids are constantly being mixed until the plugging fluid settles on top of the packer and cures at bottomhole temperature. The yield and maximum compressive strength of the solid plugs were analyzed to note any deterioration on mechanical strength by contamination. To address the effectiveness of dropping 7,000 ft in casing annulus, a new method was analytically and experimentally studied as an attempt to reduce the material losses during the fall. The method required studying the vitrification point of the epoxy to allow the formation of solid beads that liquefy at bottomhole temperature.

CHAPTER II

LITERATURE REVIEW

Epoxy-based resins are not new to the petroleum industry; they have been used for sand consolidation, resin coated proppants, remedial casing procedures, formation plugging and many other applications. For example, Kabir et al. discuss the use of resins and elastomers in water and gas shutoff applications. Thermosetting resins and elastomers are used because they have sufficient physical strength to seal fractures, perforations, and channels. Among resins, phenolic and epoxy resins are two of the types used. Conventional phenolic resin, or phenol-formaldehyde resin, may be formed by step-polymerization of phenol and formaldehyde forming a Resole as shown in **Fig. 2** (Peng and Riedl 1995). This reaction can be assisted by heating, but is slow and can be considered stable at room temperature. An acid or base catalyst is added before pumping which accelerates the reaction in the liquid and allows it to solidify at bottomhole temperature. Bottomhole temperature and pumping time should be known, to avoid polymerization of the fluid too soon or occurring too slowly (Kabir 2001). Epoxy resins are another type of thermosetting resin, especially popular in the aircraft industry. Epoxies are also common in construction and in the manufacture of composite materials with fiberglass and carbon-fiber. It consists of an epoxy group and a hardener. The hardener reacts with the epoxy, causing it to polymerize into a hard, inert plastic. Typically, epoxy is a product of the reaction between epichlorohydrin and bisphenol A, as represented in **Fig. 3**, and a common hardener is diethylenetriamine (Kabir 2001).

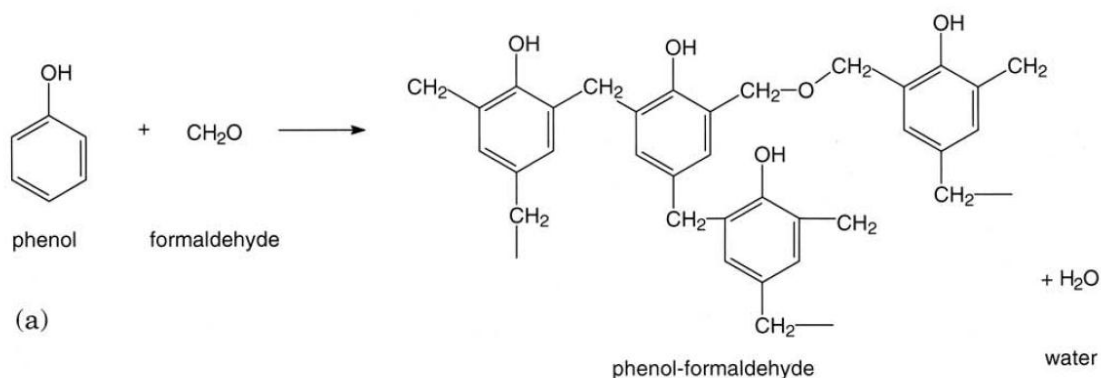


Fig. 2—The structure of a phenol-formaldehyde (Peng and Riedl 1995)

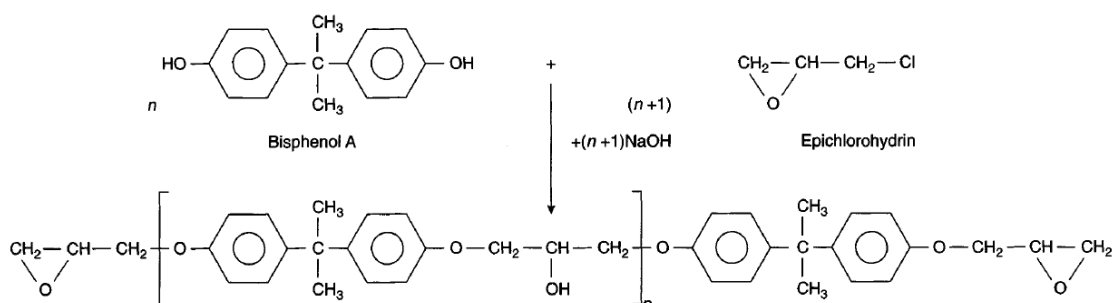


Fig. 3—Synthesis of a Bisphenol A based epoxy resin (Irfan 1998)

A patent by Ng et al. discusses the use of epoxy resin used to repair casing when it is damaged or corroded by wellbore fluids. The process described in the patent involves under-reaming the damaged section of casing and placing a retrievable packer right under the target zone, to create a surface for the epoxy to settle on. The epoxy resin mixture with hardener is then placed on top of the packer and flows into the thief zone, then forms a hardened solid underwater. The resin is typically placed with a dump bailer or through tubing squeeze in the target zone, both of these placement methods are not

suitable for the application intended herein. The solid plug formed can then be milled out to the same diameter as the casing, to form a resinous casing, as shown in **Fig. 4**. The patent explains that in wellbores at depths in excess of 5,000 ft, an environment of high temperature, high pressure, and corrosive chemicals will be encountered, which necessitates the repair in this manner. Often the wellbore is filled with materials, or brines, which deteriorate the integrity of most zonal isolation fluids. Hydrocarbons, water, saltwater, and other materials such as pipe dope, can cause the plugging fluid to deteriorate and lose effectiveness. In addition, during the time these plugging fluids are being pumped, the fluid will begin to harden during the operation such that the zonal isolation operation cannot be completed (Ng 1995). It is important to understand the cure process of the fluid in question and the effect of wellbore chemicals on the effectiveness of the plug.

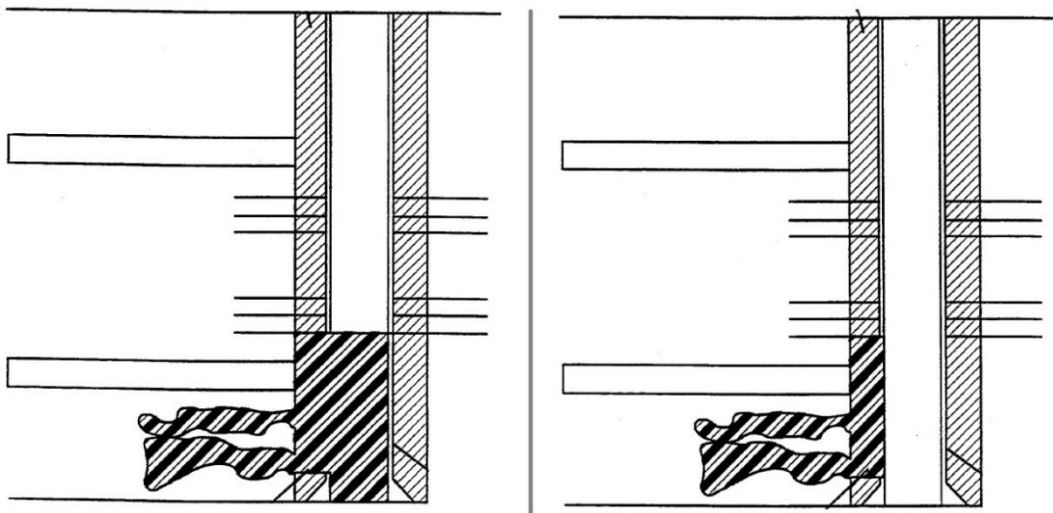


Fig. 4—Placing the epoxy resin in the thief zone and allowing it to cure, then milling out the hardened solid to the same inner diameter of the casing (Ng 1995)

ULTRA SEAL[®]-R, by Professional Fluid Services, is an epoxy-based resin that has been used in applications similar to the application discussed in this thesis and is the main material used for this research. In June of 2005, ULTRA SEAL[®]-R was used on Chevron's Vermillion 31 platform, to seal a leaking packer in an offshore production well without the use of a rig. The fluid was required to fall several feet in seawater and settle on top of the packer. 168 gallons of the fluid were loaded into the annulus along with 9 bbls of seawater. After 14 hours of settling time and 24 hours of curing time the plug was tested at 1,000 psi without pressure losses. PFS has applied ULTRA SEAL[®]-R in several other wells in the Gulf of Mexico, one of these was W&T Offshore-Ship Shoal 349, Well A7. The objective of the operation was to seal micro annular gas migration. To achieve the objective, two plugs were required. Prior to pumping Liquid Bridge Plug[®] (another name for ULTRA SEAL[®]-R), the well was cleaned by circulating it with seawater. Prior to pumping the first plug, 15 ft of sand were pumped to the bottom then 7 bbls of Liquid Bridge Plug[®] were circulated down on top of the sand. The well was tested to 600 psi with no pressure loss over 24 hours. 12 bbls of Liquid Bridge Plug[®] were circulated to form the second plug and the well was tested to 800 psi with no pressure loss over 48 hours (P.F.S 2007).

Table 1—EPOXY FALL RATE IN 30 FT OF WATER (After El-Mallawany 2011)

Annulus	Epoxy Density, ppg	Angle, degrees	Fall Rate, ft/min	Material Loss, %
6" - 0"	11.5	0	39.46	18.8
6" - 0"	13.2	0	41.71	19.3
6" - 0"	13.2	0	41.71	16.4
6" - 0"	14.7	0	50.34	28.4
6" - 0"	13.2	30	91.25	21.9
6" - 0"	13.2	45	85.88	27.7
6"-1.9"	11.5	0	36.5	24.9
6"-1.9"	13.2	0	42.94	25.8
6"-1.9"	14.7	0	60.83	31.4
6" - 3.5"	11.5	0	36.5	25.9
6" - 3.5"	13.2	0	44.24	26.3
6" - 3.5"	14.7	0	56.15	32.3

El-Mallawany developed an experimental apparatus to determine the fall rate of epoxy in a column of water, and measure the material losses during the fall. The apparatus involved a 30-ft column of clear PVC pipe mounted on a metal support structure. The structure is hinged and can be tilted at any angle between vertical and horizontal. Epoxy was dumped into the top of the pipe and collected at the bottom. The results of the experiments are presented in **Table 1** above, which shows significant trends in terms of annulus size, inclination, density, and material loss. It was found that the size of the annulus had no effect on the terminal velocity, where it averaged around 37.5-, 41.7-, and 55.8-ft/min for 11.5-, 13.2-, and 14.7-ppg formulations, respectively. On the other hand, a smaller annulus caused more material buildup on the walls, resulting in losses of up to 32.3%. It was also noted that in sloping columns, both fall rate and material losses increase, compared to a vertical column. **Fig. 5** shows the

behavior of the epoxy as it falls through the water column. The fluid broke down into smaller droplets and spread through the water, but, due to the difference in densities, the epoxy fell to the bottom of the pipe and settled as one mass (El-Mallawany 2011).



Fig. 5—Epoxy breaking down into smaller droplets and spreading in a column of water (El-Mallawany 2011)

CHAPTER III

PRIMARY OBJECTIVES

1. Determine if there is a reduction in yield strength, fracture strength, or ultimate strength of cured epoxy-based resin as a result of being mixed for one hour with seawater, oil, or pipe dope during the 7,000-ft fall in the contaminant. Determine if any of the contaminants deteriorate the resin's integrity, to the extent of causing a 25% reduction in fracture strength compared to pure epoxy-based resin.
2. The application discussed in this thesis requires the resin to cure in the presence of wellbore chemicals. It is important to study the cure process of epoxy resin in the presence of seawater, oil, and pipe dope, to understand the changes in terms of cure time and level of gelation relative to pure resin. During a 6-hour cure time, the criteria for defining a significant change from the cure process of pure resin are a difference of 2 hours in the cure time, or a reduced level of gelation of 4 at 6 hours.
3. Determine whether the vitrification point of epoxy resins successfully allows the formation of solid beads without gelation. Secondly, determine whether the vitrified solid beads can be stored for a period of time greater than double the 6-hour cure period of the resin. Finally, determine whether the solid beads can be devitrified at wellbore temperature and reconsolidate into one mass and cure.

4. Determine if the compressive strength of the reconsolidated resin solid to can be an improvement over Portland cement, specifically creating an increase in strength of up to 50%.
5. Analyze the operational cost savings by comparing the use of vitrified resin beads to conventional cement. Determine cost savings created by reducing the material losses, due to using vitrified epoxy resin beads in place of pumping liquid epoxy in a 7,000-ft application.

CHAPTER IV

MECHANICAL STRENGTH TESTS

Background

Epoxy-Based Resin

Epoxy resins are compounds with more than one ethylene oxide. These resins are called “thermosetting” resins, due to their ability to harden, or cure, with increasing temperature. Typical construction applications for epoxies require the resin to be mixed with other compounds or resins to achieve the desired characteristics of the thermoset (Irfan 1998). In some cases these resins are mixed with phenol-formaldehyde based resins.

The resin used in this thesis consists of Part A, Part B, and a diluent mixed in the ratios shown in **Table 2**. The content of Part A includes phenol-formaldehyde, Diglycidylether and 1-chloro-2,3-epoxypropane, also known as epichlorohydrin. Phenol-formaldehyde is stable at room temperature, until it reacts at 200°F. The reaction is a step-growth polymerization, where phenol reacts with formaldehyde and forms a hydroxymethyl phenol. The hydroxymethyl group can react with another phenol and create a methylene bridge, or react with another hydroxymethyl group to form a diphenol, called bisphenol F. Bisphenol F is an important monomer that is present in epoxy resins, and it can further react with itself to create larger phenol oligomers. Diglycidylether and epichlorohydrin, are epoxy resin components that react with the

hardener triethylenetetramine, TETA, from part B causing it to polymerize into a hard, inert plastic (Kelland 2009).

Table 2—MIX RATIOS FOR ULTRA SEAL-R

<u>Component</u>	<u>Weight</u>	<u>Volume</u>	<u>Density</u>	
	g	mL	g/mL	ppg
Part A	2.89	2.42	1.19	9.97
Diluent	0.29	0.3	0.97	8.07
Part B	0.87	0.91	0.96	7.98

Pipe Dope

Pipe dope is used as a thread lubricant, and thread sealing compound for casing and tubing threads. The main use is to make a joint leak-proof and pressure-tight. While most pipe threads are machined to form an interference fit with proper assembly, some machining and finishing variances will result in a less than 100% fit. Pipe dope is applied to all casing and tubing joints prior to assembly, to ensure minor gaps will be filled and any potential leaks blocked. As a result of the frequent use in the assembly of casing and tubing, pipe dope is one of the most prominent materials in production tubing and annuli (Gougler Jr. et al. 1985; Loewen et al. 1990; Nasr-El-Din et al. 2002). All the pipe dope compounds used in these experiments are products of Bestolife Corporation and conform to API RP 5A3 with the exception of “ZN 18”, a zinc-based nonmetal compound. “ZN 18” was recommended for testing by the company representatives because of its popularity in the industry as a thread compound suitable for storage and light duty use. The main components of the pipe dope compounds are a petroleum grease

mixture and either metallic or nonmetallic particles. “OCTG” is a black-copper compound which contains zinc, graphite, copper and other nonmetallic additives. “2000” is a black-copper colored compound with lime, inert nonmetallic solids, and less than 4 wt % copper. “API Modified” is a black-copper colored compound with powdered graphite, copper flakes, lead powder, and zinc dust. “4010 NM” is a gray compound with graphite, calcium compounds, talc, and titanium dioxide. “Metal Free” is a black compound with synthetic and amorphous graphite, Teflon[®], and other nonmetallic additives. The composition of the mentioned pipe dope compounds is presented in **Table 3**.

Table 3—6 TYPES OF "BESTOLIFE" PIPE DOPE

Pipe dope	Composition (with petroleum grease mixture)
OCTG	Zinc, graphite, copper, & nonmetallic additives
2000	Lime, inert nonmetallic additives, & copper
API Modified	Graphite, zinc, copper, lead, & lime
4010 NM	Graphite, talc, calcium compounds, titanium dioxide
ZN18	Zinc
Metal Free	Synthetic and amorphous graphite, Teflon [®] , nonmetallic additives

Properties of Wells in the Gulf of Mexico

This research focuses on wells in the Gulf of Mexico; therefore it is necessary to perform all experiments in similar conditions. In offshore wells, seawater is present in abundance. The seawater mixture used in the experiments in this thesis, included, in decreasing weight percent: sodium chloride, magnesium chloride hexahydrate, sodium sulfate, calcium chloride dihydrate, and sodium bicarbonate, as listed in **Table 4**. Model wells will be chosen with a packer depth of approximately 7,000 ft TVDSS. At this

depth the temperature is approximately 200°F based on the upper end of the temperature gradient scope which ranges between 0.8°F/ft and 1.9°F/ft as shown in **Fig. 6** (API 1999).

Table 4—COMPOSITION OF SEAWATER

<u>Salt</u>	<u>g/100mL of H₂O</u>
NaCl	3.839
CaCl ₂ ·2H ₂ O	0.244
MgCl ₂ ·6H ₂ O	1.906
Na ₂ SO ₄	0.526
NaHCO ₃	0.027

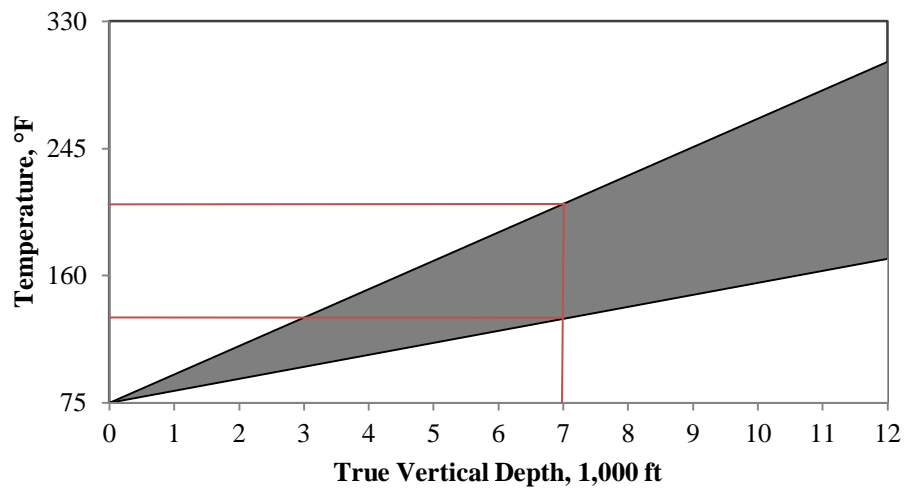


Fig. 6—The approximate temperature increase per 1,000 ft True Vertical Depth Subsea based on a 0.8 °F/100ft and 1.9 °F/100ft rate (data from API 1999)

Mechanical Strength

Hooke's Law

Hooke's Law of Elasticity states that the extension (or contraction) of a spring is directly proportional to the load applied on it. Many materials obey this law, as long as the load does not exceed the material's elastic limit. Hooke's Law is represented by

$$F = kx$$

where F is the applied load, x is the extension or contraction, and k is the proportionality constant.

Stress-Strain Curves

The mechanical strength of a material is largely defined by its internal stresses in the material. Knowledge of these stresses is essential in a safe design. When compressive or tensile tests are carried out on cylindrical specimens with different cross-sections of the same material, the breaking loads are found to be proportional to the cross-sectional area A of the specimen. This is because the strength of the material is determined by the intensity of the force on the normal cross-section, and not on the net force P . This intensity is known as the compressive stress σ , in the case of compressive loading. The compressive stress of a cylindrical specimen is defined as

$$\sigma = \frac{P}{A}$$

where P is the net axial force applied on the normal cross-sectional area A of the cylinder, as shown in **Fig. 7**.

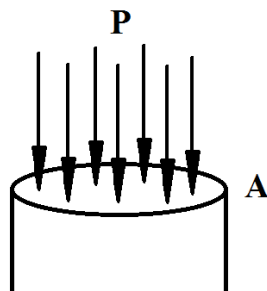


Fig. 7—Applied axial compression force P on the normal cross-sectional area A of a cylindrical specimen

Strain, by definition, is a measure of the distortion of the material under a compressive or tensile load. The compressive strain is a non-dimensional quantity, and is the ratio of the contraction of the material l to the original length L_0 of the specimen; the compressive strain ε is defined as

$$\varepsilon = \frac{l}{l_0}$$

Many characteristics can be deduced from a compression test by creating a stress-strain curve. These characteristics are a more convenient method of comparing materials, than using loads and contractions. Typically, different brittle materials follow the same general trend, shown in the stress-strain curve in **Fig. 8**. The initial portion of the stress-strain curve is linear, where the material acts elastically obeying Hooke's law, and no permanent distortion occurs if the load is removed during this period. With increasing loads, the material begins to deform plastically up to the breaking point (Case et al. 1999).

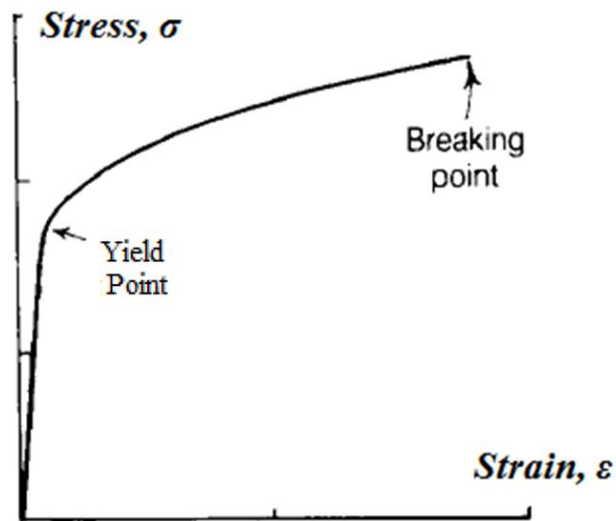


Fig. 8—Stress-Strain curve for a brittle material (after Case et al. 1999)

Brittle materials are classified as materials that exhibit relatively little contraction at failure. In contrast, materials such as mild steel and synthetic polymers show significant deformation before failure. These materials are classified as ductile materials. Ductile materials have the same general trend as brittle materials on a stress-strain curve but differ in some key characteristics. The stress-strain curve, in **Fig. 9**, obeys Hooke's law where the slope is linear and elastic up to a point called the yield point. Loading the specimen past this point exhibits a drastic decrease in the slope of the curve, where the stress decreases then remains constant while strain continues to increase. The material becomes strain-hardened, and the stress again begins to increase until failure. The point of highest stress, the ultimate stress, may be reached before or at fracture.

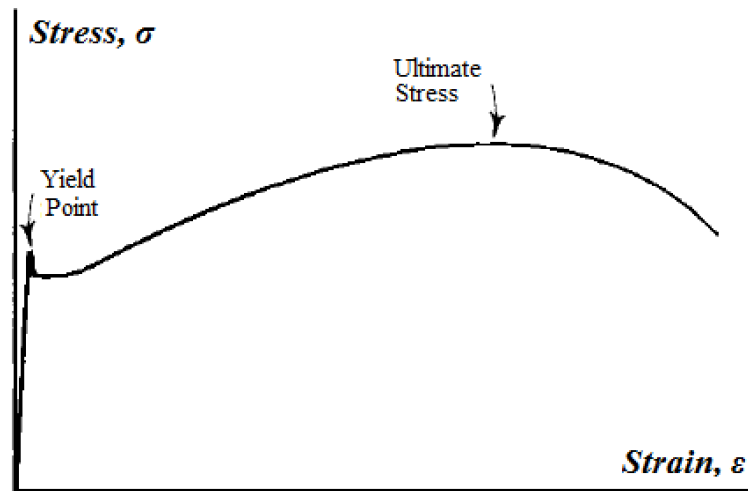


Fig. 9—Stress-Strain curve for a ductile material (after Case et al. 1999)

In certain cases, a material fractures at the yield point but continues to deform while maintaining a constant stress level. Wei et al. describe such materials as having crack tolerance. The residual stress due to crack tolerance allows the material to withstand the load until it eventually fails completely at the rupture point (Wei 2010). The rupture point is defined on a stress-strain graph by a sudden drop in stress.

Failure Modes

Ductile and brittle materials fracture in different manners. Brittle materials tend to fail with a fracture that extends in a diagonal plane in the specimen, as shown in **Fig. 10**, or crumble into smaller pieces. On the other hand, ductile materials experience greater contraction accompanied by radial expansion along the specimen resulting in a barrel-like shape as shown in **Fig. 11**.

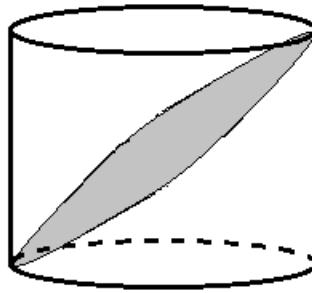


Fig. 10—Failure showing a fracture in a diagonal plane due to compressive loading on a specimen of a brittle material

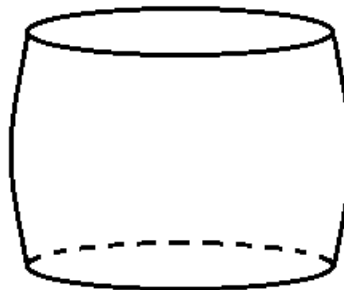


Fig. 11—Barrel-like failure due to compression on a specimen of ductile material

Objectives

Determine if there is a reduction in yield strength, fracture Strength, or ultimate strength of cured epoxy-based resin, as a result of being mixed for one hour with seawater, oil, or pipe dope during the 7,000 ft fall in the contaminant. Determine if any of the contaminants deteriorate the resin's integrity to the extent of causing a 25% reduction in fracture strength compared to pure epoxy-based resin.

Procedure

The parts of epoxy-based resin were mixed and allowed to cure in an oven under a simulation of the plugging fluid falling 7,000 ft in the wellbore. This was carried out by mixing the resin with each contaminant at wellbore conditions before allowing it to settle and cure in the oven. The resin was prepared following the steps mentioned below:

1. Set the oven temperature to 200°F and allow it to reach steady state.
2. Prepare the first portion of the resin formulation by thoroughly mixing the Part A resin and diluent in a beaker based on the ratios in Table 2 above.
3. Mix in Part B of the resin formulation based on the ratios in Table 2 above.

The samples simulating the 7,000 foot drop in the wellbore require the resin to be mixed with the contaminant for a certain time period under certain temperatures to replicate wellbore conditions. Preparation of the mixture requires the use of a heat-plate magnetic stirrer, for the setup of a water bath and to create turbulence in the beaker. The temperature in the water bath is linearly increased from 80°F to the bottom-hole temperature, 200°F, for one hour, roughly matching the fall rate of the resin. The procedure followed to prepare samples of resin mixed with contaminants is listed below:

4. Prepare a 150-mL batch of resin.
5. Set up a hot water bath by placing a 5,000-mL glass container on a magnetic stirrer/hot plate combination device.

6. Fill up approximately 400 mL of water and heat the water to 80°F.
7. Place the beaker of resin in the hot water.
8. Mix in the contaminant using a magnetic stirrer rod. Use quantities of contaminants based on **Table 5**.
9. Cover the large glass container and allow the fluid to mix for one hour while ramping the temperature of the water bath from 80°F to 200°F
10. Distribute the fluid into 50-mL Ultra-High Performance Centrifuge Tubes with 45 mL of fluid per tube.

Table 5—MIX RATIOS OF CONTAMINANTS IN RESIN			
	Mass of Resin, g	Mass of Contaminant, g	wt % Contaminant
Seawater	111	102	91.9%
ZN18	167	10	5.7%
API	167	9	5.6%
2000	167	10	6.0%
OCTG	167	10	6.2%
Metal Free	167	11	6.4%
4010NM	167	11	6.7%
Oil	80	57	72.0%

The strength of a material is a relation of the load and dimension of the sample. If the ratio of height to diameter of the specimen is equal to or less than 1.75, then the correction factor in **Table 6** must be applied to the stress values obtained (ASTM 1999a). It is important for uniaxial compression tests to maintain a load vector parallel to the axis of the sample being tested. As a result, the samples are required to have ends that are parallel to each other and the surfaces of the compression machine. The ends are also required to be square with the sides of the cylinder to ensure uniform loading and

deformation. The following list describes the steps necessary to achieve these requirements:

11. Remove the cured solid samples from the 50-mL Ultra-High Performance Centrifuge Tubes.
12. Use a band-saw to cut off the conical end of the sample and to cut the samples into two 1-inch long cylinders.
13. Sand the ends of the samples on a disc sander to ensure parallel ends to the sample as well as to smooth off the surface for an adequate compression test surface.
14. Measure the height and average diameter of each specimen.
15. Check each sample for its conformance to the requirement of parallel top and bottom ends. Any sample that does not meet the specifications is unsuitable for testing.

<u>L/D</u>	<u>k, correction factor</u>
1.75	0.98
1.5	0.96
1.25	0.93
1	0.87

The compression tests were run using an Instron 4206, **Fig. 12**, connected to a computer running a Labview data acquisition program. For each run, the machine was allowed to apply a load on the sample until the sample failed or the load reached the load limit of 30,000-psi. A sample failing is indicated by a sudden drop in the measured load.

The following steps list the directions used to run the compression tests and collect the data points:

16. Turn on the Instron 4206.
17. On the control panel displayed in **Fig. 13**, hit “Load Cal” then “Enter”
18. Hit “Load Bal” then “Enter”
19. Hit “GL reset”
20. Hit “Speed” and set it to 0.2 inches per minute.
21. Launch the Labview program.
22. Start data acquisition by running the Labview program.
23. Hit the “Down” button to start the Instron.
24. Stop the machine when the sample fails or reaches the load limit of 30,000-psi.



Fig. 12—The Instron 4206 used for compression tests with a load limit up to 30,000 psi



Fig. 13—The control panel for the Instron 4206

Results and Discussion

Pure Epoxy-Based Resin

The compression tests on samples of pure epoxy resin produced the expected stress-strain graph of a ductile material as shown in **Fig. 14**. The slope of the curve increases linearly up to, approximately, 13,900 psi and a strain of 0.11, where the stress dropped and remained relatively constant then gradually increased. Every specimen of pure resin experienced a gradual increase in stress until failure. The point of failure is the point of maximum stress, or ultimate stress, and averaged at 19,800 psi.

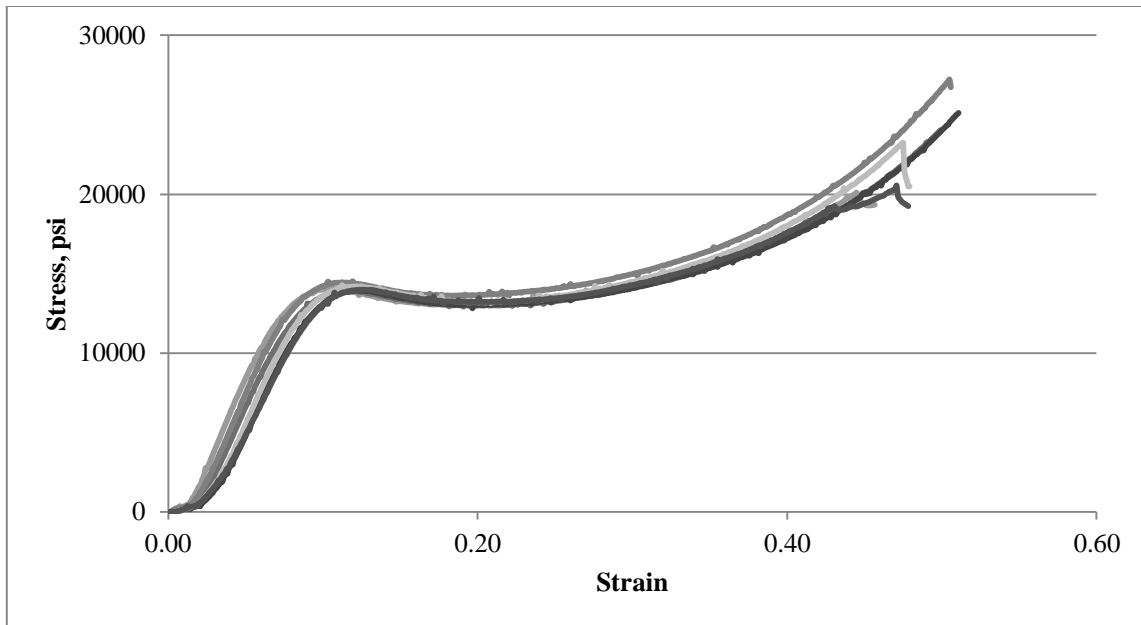


Fig. 14—The stress-strain curve from 6 experiment runs for pure epoxy-based resin, tested under compression until failure

The resin specimens were clear, yellow solid cylinders, as shown in **Fig. 15**. Barreling of the specimen was initiated at the yield point. It then continued to withstand loads until the first crack propagated at the ultimate stress point. Once cracks formed, the specimen lost its integrity and lost its ability to withstand loads resulting in the crack pattern in Fig. 15.



Fig. 15—A specimen of pure epoxy-based resin before and after the compression test

Seawater Brine

The resin was mixed with seawater for one hour, as described in the procedure section above. Before mixing the two fluids it was obvious the fluids were not miscible, as can be seen in the clear separation in **Fig. 16**.



Fig. 16—The separation of resin and seawater brine is apparent due to the fluids being immiscible

After mixing the fluids for an hour and linearly increasing the temperature up from 80°F to 200°F, the resin and brine fluids formed an emulsion as can be seen in **Fig. 17**.



Fig. 17—An emulsion of resin droplets in seawater brine during and after mixing for one hour prior to curing

Once the mixture was prepared and ready to be transferred to the oven to cure, the fluid was distributed among the centrifuge tubes. The epoxy resin droplets began separating out of the emulsion and a separation between the two fluids was again appearing, but only when settled in the oven for more than 15 minutes. The separation can be seen in **Fig. 18**. Over the first hour, the resin had settled at the bottom of the tubes and continued the cure process until fully cured.

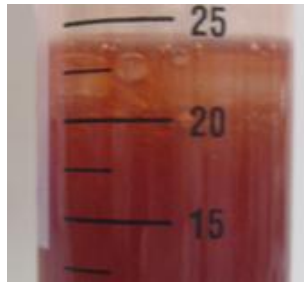


Fig. 18—Epoxy and seawater brine mixture after being mixed for an hour then settling for approximately 15 minutes in a 200 °F oven

Once the samples were fully cured, the compression tests were performed as described in the procedure section. The compression tests on samples of epoxy-resin mixed with seawater produced a stress-strain graph of a ductile material, as shown in **Fig. 19**. Initially, the slope of the curve increased linearly then decreased at the yield point, as it did for pure epoxy resin. Similar to pure epoxy resin, the yield strength and maximum compressive strength were two distinct points on the stress-strain graph. In addition, the maximum compressive strength corresponded to the fracture strength of the specimens. After the yield point, the stress dropped slightly then gradually increased. The specimens continued to deform until fractures propagated through the samples and resulted in the fracture pattern shown in **Fig. 20**.

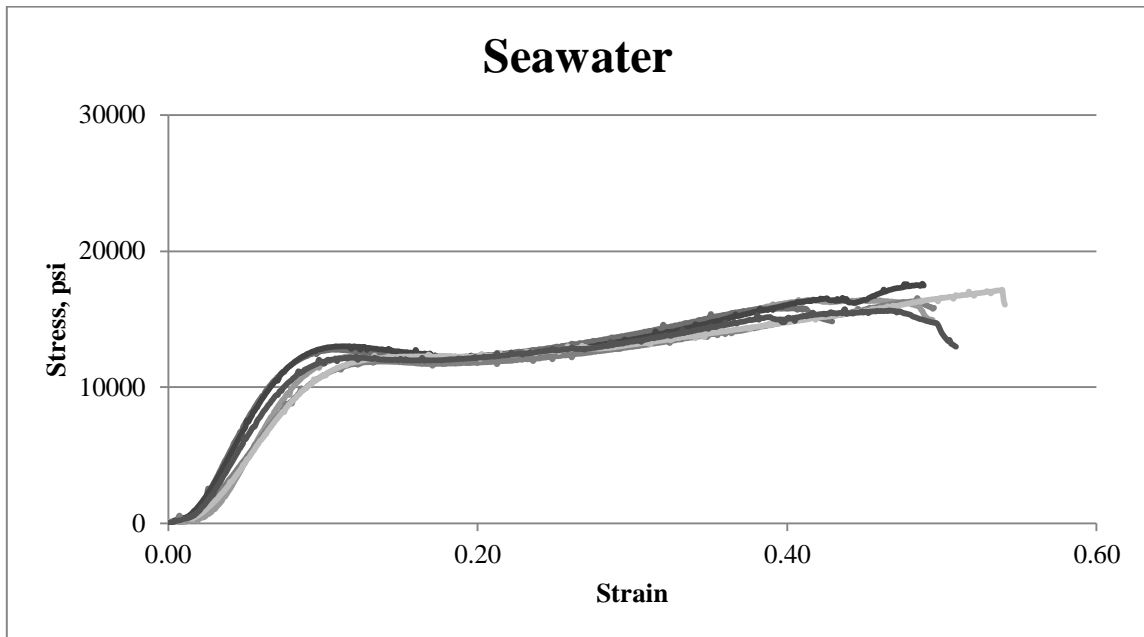


Fig. 19—The stress-strain curve from different experiment runs for epoxy-based resin with seawater brine, tested under compression until failure



Fig. 20—A specimen of fully cured resin mixed with seawater brine before and after the compression test

Pipe Dope

The different types of pipe dope were mixed in with the resin as described in the procedure section above. Initially, the pipe dope added to the solution settled at the bottom of the beaker, due to its greater density. Through mixing and heating, the liquid portion of the pipe dope mixed with the resin, and the solid particles were suspended in the fluid due to the turbulence of mixing. After the preparation stage, the samples were distributed over the centrifuge tubes and allowed to cure in the oven. By remaining stationary in the oven, the solid particles settled to the bottom of the tubes while the liquid portion of the pipe dope remained in the mixture.

ZN18

ZN 18 is a zinc-based nonmetal compound popular in the industry for storage and light duty use, despite not being rated per API RP 5A3. The ZN18 thread compound, shown in **Fig. 21**, is a grey compound of fine grey zinc dust held together by the organic grease having a yellow-green appearance. The fully cured mixture in **Fig. 22** shows the zinc particles collected at the bottom of the tube while the grease component of ZN18 pipe dope remained in the mixture.



Fig. 21—ZN18 thread compound



Fig. 22—The fully cured sample of resin mixed with ZN18 pipe dope

Once the samples were fully cured, the compression tests were performed as described in the procedure section. The compression tests on samples of epoxy resin mixed with ZN18 pipe dope produced the stress-strain graph shown in **Fig. 23**. Initially, the slope of the curve increased linearly then the slope decreased at the yield point. It is important to note that, unlike the pure resin samples, these samples fractured at the yield point, but maintained a constant stress after the yield point while the sample continued to

deform. The samples displayed the barreling effect at the yield point, which is an effect definitive of ductile failure, and formed the fracture pattern shown in **Fig. 24**.

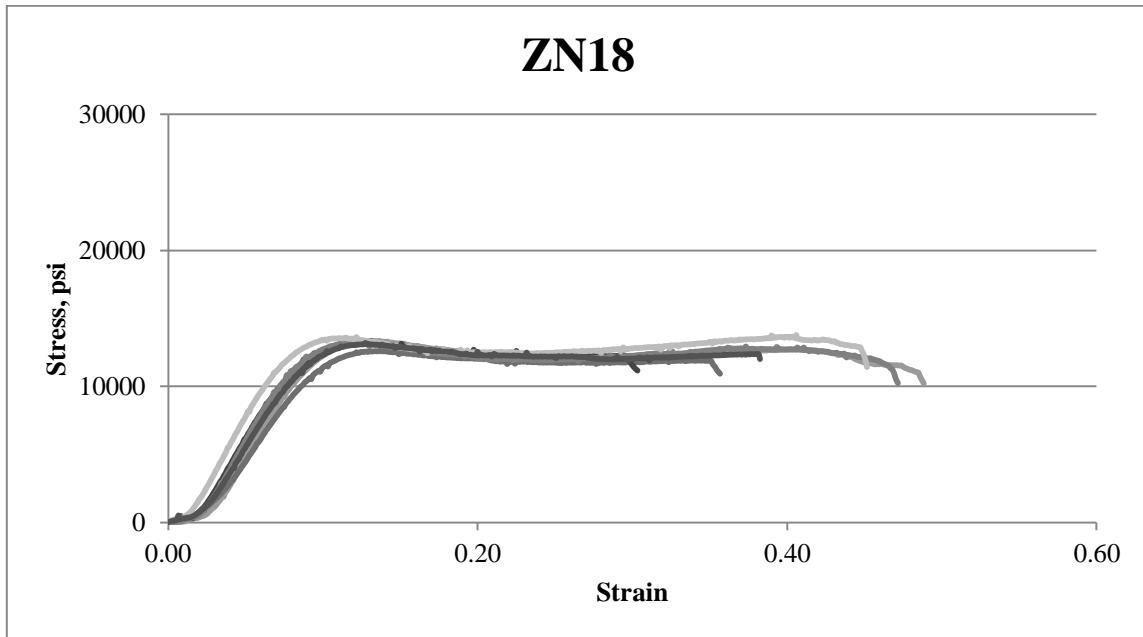


Fig. 23—The stress-strain curve from different experiment runs for epoxy-based resin with ZN18 pipe dope, tested under compression until failure



Fig. 24—A specimen of fully cured resin mixed with ZN18 pipe dope before and after the compression test

API-Modified

API-Modified is a black-copper colored compound with powdered graphite, copper flakes, lead powder, and zinc dust which is rated per API RP 5A3. The API-Modified compound shown in **Fig. 25** is a dark brown/copper colored compound, held together by organic grease having a yellow-green appearance. The fully cured mixture in **Fig. 26** shows the grease component of API-Modified pipe dope mixed with the resin, and distributed solid flakes throughout the length of the sample.



Fig. 25—API-Modified pipe dope compound



Fig. 26—The fully cured sample of resin mixed with API-Modified pipe dope

Once the samples were fully cured, the compression tests were performed as described in the procedure section. The compression tests on samples of epoxy resin mixed with API-Modified pipe dope produced the stress-strain graph shown in **Fig. 27**. Initially, the slope of the curve increased linearly then the slope decreased at the yield point. Similar to ZN18 samples, these samples fractured at the yield point and maintained a constant stress after the yield point while the sample continued to deform. The samples displayed the barreling effect at the yield point, which is an effect definitive of ductile failure, and formed the fracture pattern shown in **Fig. 28**.

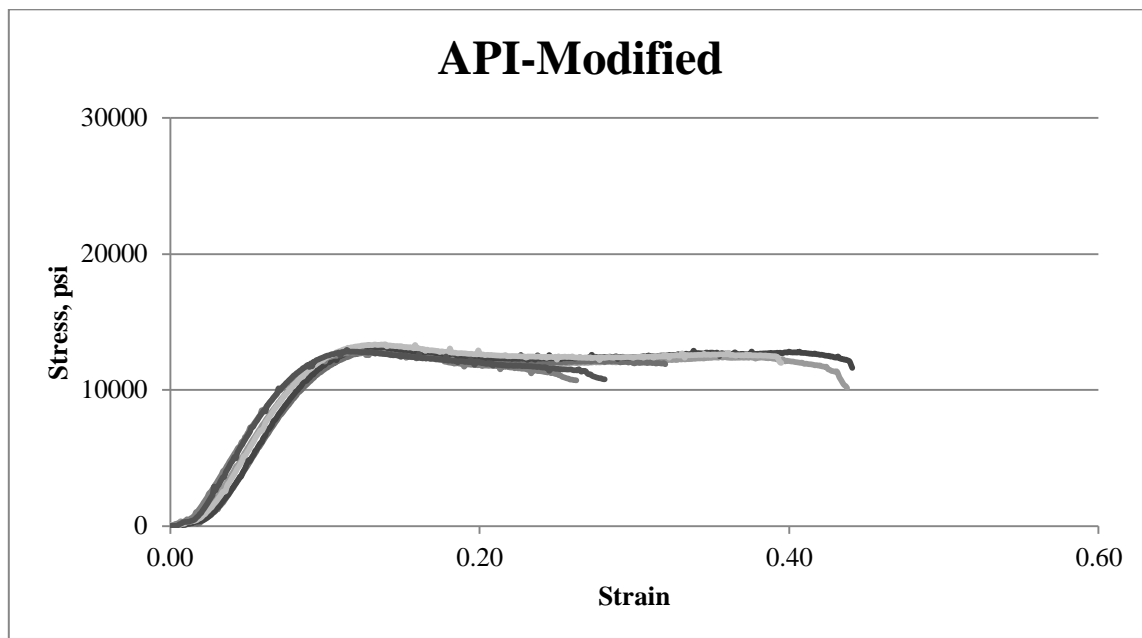


Fig. 27—The stress-strain curve from different experiment runs for epoxy-based resin with API-Modified pipe dope, tested under compression until failure

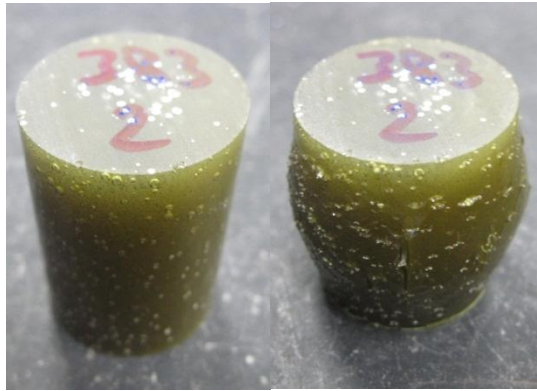


Fig. 28—A specimen of fully cured resin mixed with API-Modified pipe dope before and after the compression test

2000

2000, rated per API RP 5A3, is a black-copper colored compound, as shown in **Fig. 29**, with lime, inert nonmetallic solids, and less than 4 wt % copper. The solid particles of 2000 compound are held together by organic grease having a yellow appearance. The fully cured mixture in **Fig. 30** shows the grease component of 2000 pipe dope mixed in with the resin and distributed black solid flakes throughout the length of the sample.



Fig. 29—2000 pipe dope compound



Fig. 30—The fully cured sample of resin mixed with 2000 pipe dope

Once the samples were fully cured, the compression tests were performed. The compression tests on samples of epoxy resin mixed with 2000 pipe dope produced the stress-strain graph shown in **Fig. 31**. These samples fractured at the yield point, and maintained a constant stress after the yield point while the sample continued to deform. The samples displayed the barreling effect at the yield point, which is an effect definitive of ductile failure, and formed the fracture pattern shown in **Fig. 32**.

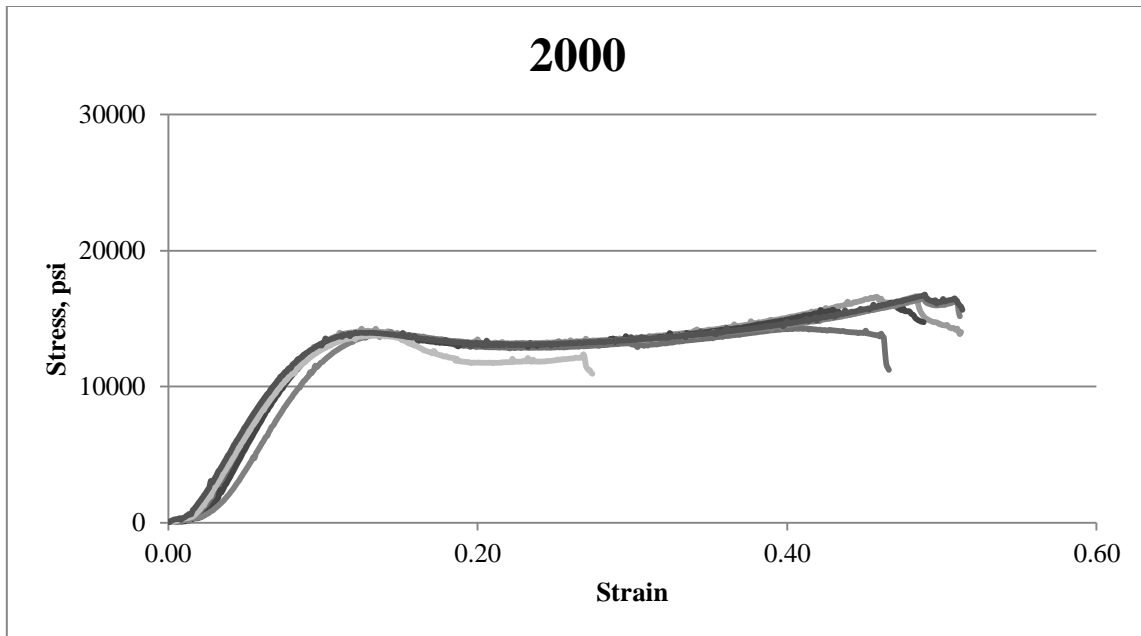


Fig. 31—The stress-strain curve from different experiment runs for epoxy-based resin with 2000 pipe dope, tested under compression until failure



Fig. 32—A specimen of fully cured resin mixed with 2000 pipe dope before and after the compression test

OCTG

OCTG, rated per API RP 5A3, is a black-copper compound, as shown in **Fig. 33**, which contains zinc, graphite, copper and other nonmetallic additives. The fully cured

mixture in **Fig. 34**, shows the grease component of OCTG pipe dope mixed in with the resin while solid particles in the compound settled out of solution to the bottom of the tubes.



Fig. 33—OCTG pipe dope compound



Fig. 34—The fully cured sample of resin mixed with OCTG pipe dope

The compression tests were performed on the fully cured samples of epoxy resin mixed with 2000 pipe dope, and produced the stress-strain graph shown in **Fig. 35**.

These samples fractured at the yield point and also started barreling at the yield point.

The barreling effect and the fracture pattern on the specimen are shown in **Fig. 36**.

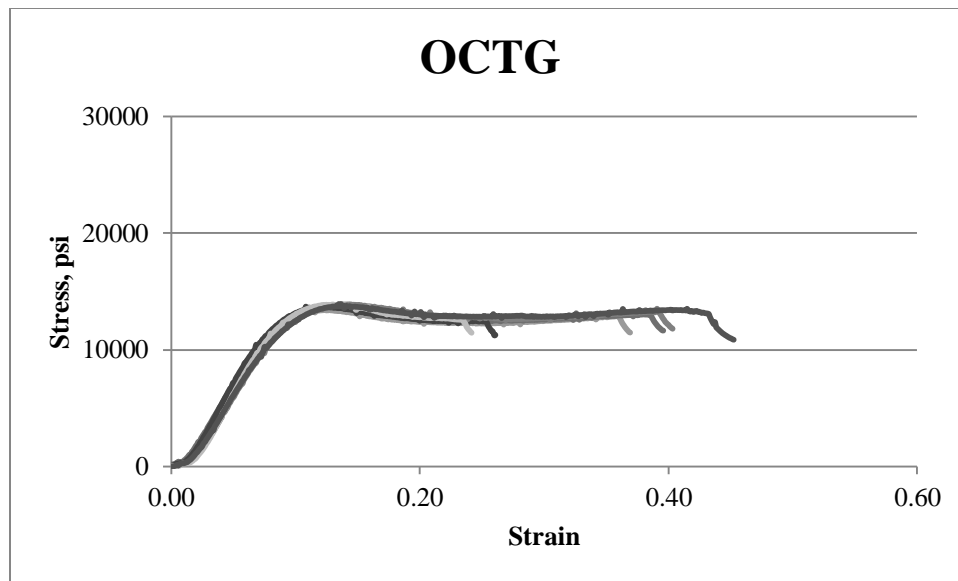


Fig. 35—The stress-strain curve from different experiment runs for epoxy-based resin with OCTG pipe dope, tested under compression until failure

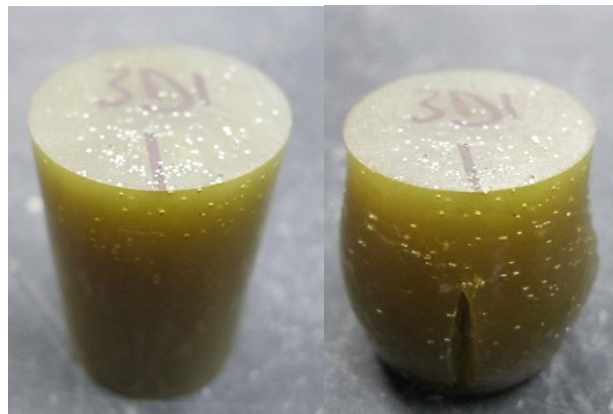


Fig. 36—A specimen of fully cured resin mixed with OCTG pipe dope before and after the compression test

Metal Free

Metal Free, rated per API RP 5A3, is a black compound, as shown in **Fig. 37**, with synthetic and amorphous graphite, Teflon[®], and other nonmetallic additives. The

fully cured mixture in **Fig. 38** shows the green grease component of Metal-free pipe dope mixed in with the resin, while the fine solid particles in the compound settled out of solution to the bottom of the tubes.



Fig. 37—Metal-free pipe dope compound



Fig. 38—The fully cured sample of resin mixed with Metal-free pipe dope

The compression tests were performed on fully cured samples of epoxy resin mixed with Metal-free pipe dope, and produced the stress-strain graph shown in **Fig. 39**. The stress-strain graph displays a yield stress and ultimate stress, but samples were observed to fracture at the yield point, an effect in brittle materials. The samples deformed elastically by barreling at the yield point, producing the fracture pattern shown in **Fig. 40**, then continued deforming and strain hardening, despite the present fractures.

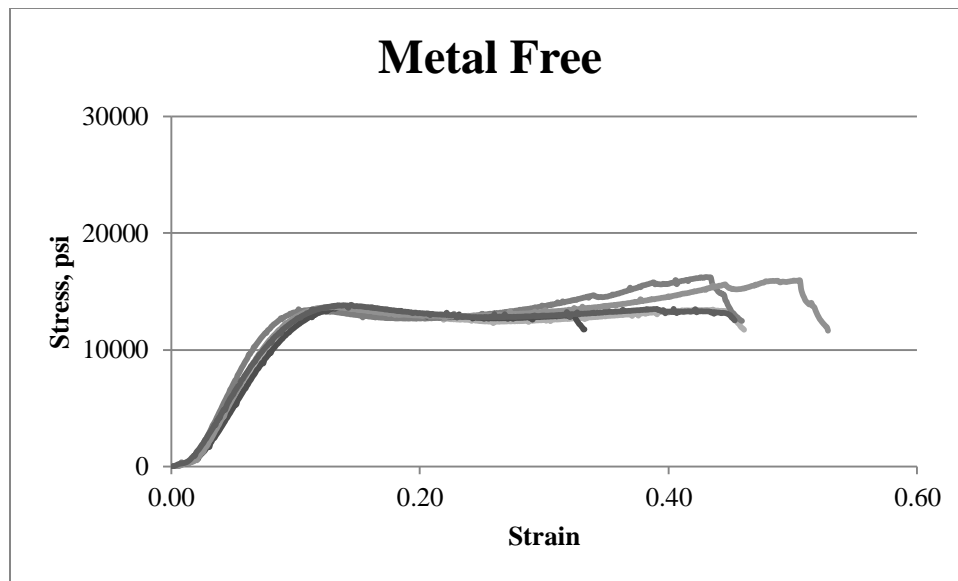


Fig. 39—The stress-strain curve from different experiment runs for epoxy-based resin with Metal-free pipe dope, tested under compression until failure

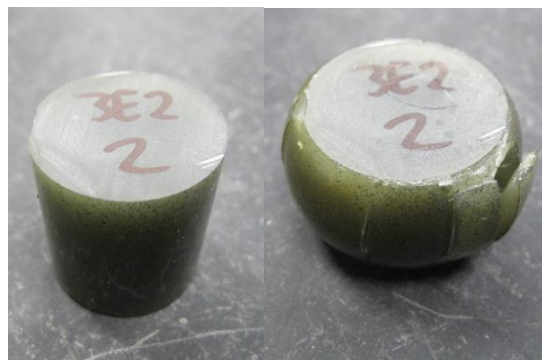


Fig. 40—A specimen of fully cured resin mixed with Metal-free pipe dope before and after the compression test

4010NM

4010NM is a gray compound, rated per API RP 5A3, containing graphite, calcium compounds, talc, and titanium dioxide. The compound in **Fig. 41** shows a grey compound held together by the organic grease having a yellow appearance. The fully

cured mixture in **Fig. 42**, shows the fine particles collected at the bottom of the tube while the grease component of 4010NM pipe dope remained in the mixture.



Fig. 41—4010NM pipe dope compound



Fig. 42—The fully cured sample of resin mixed with 4010NM pipe dope

The compression tests we performed on fully cured samples of epoxy resin mixed with 4010NM pipe dope, and produced the stress-strain graph shown in **Fig. 43**. The samples deformed by barreling at the yield point, producing the fracture pattern shown in **Fig. 44**, then continued deforming and strain hardening, despite the present fractures. The fracture strength in this case is at the yield point of the stress-strain graph.

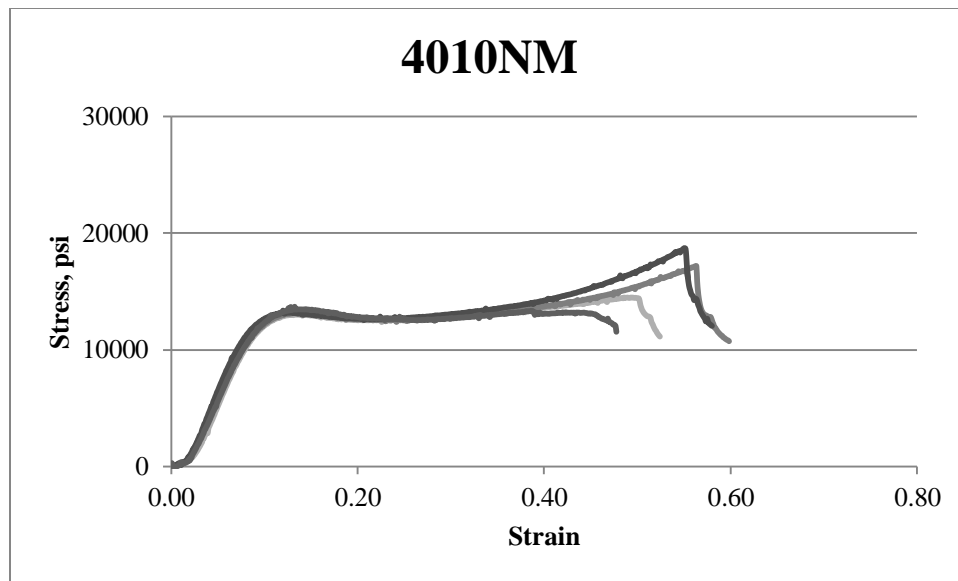


Fig. 43—The stress-strain curve from different experiment runs for epoxy-based resin with 4010NM pipe dope, tested under compression until failure

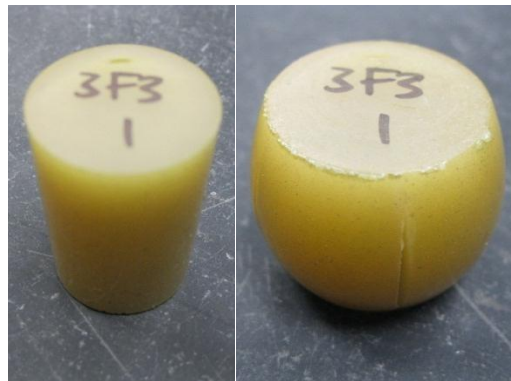


Fig. 44—A specimen of fully cured resin mixed with 4010NM pipe dope before and after the compression test

Sour Oil

Sour oil was mixed with the resin for one hour while linearly increasing the temperature from 80 °F to 200 °F as described in the procedure section above. The resin

was miscible in oil, therefore, mixing the two fluids resulted in one homogeneous fluid which was distributed over the centrifuge tubes and allowed to cure in the oven. The fully cured sample was a dark brown/black opaque solid as shown in **Fig. 45**.



Fig. 45—The fully cured sample of resin mixed with sour oil

Once the samples were fully cured, the compression tests were performed to produce the stress-strain graph shown in **Fig. 46**. The stress-strain was similar to that of pure resin, with distinct yield and maximum compressive strengths. In addition, the maximum compressive strength of these mixtures corresponded to the samples' fracture strength. At the yield point on the stress-strain graph, the samples experienced barreling then continued deformation while not forming any fractures. At the fracture point the specimens developed the shape and fracture pattern shown in **Fig. 47**.

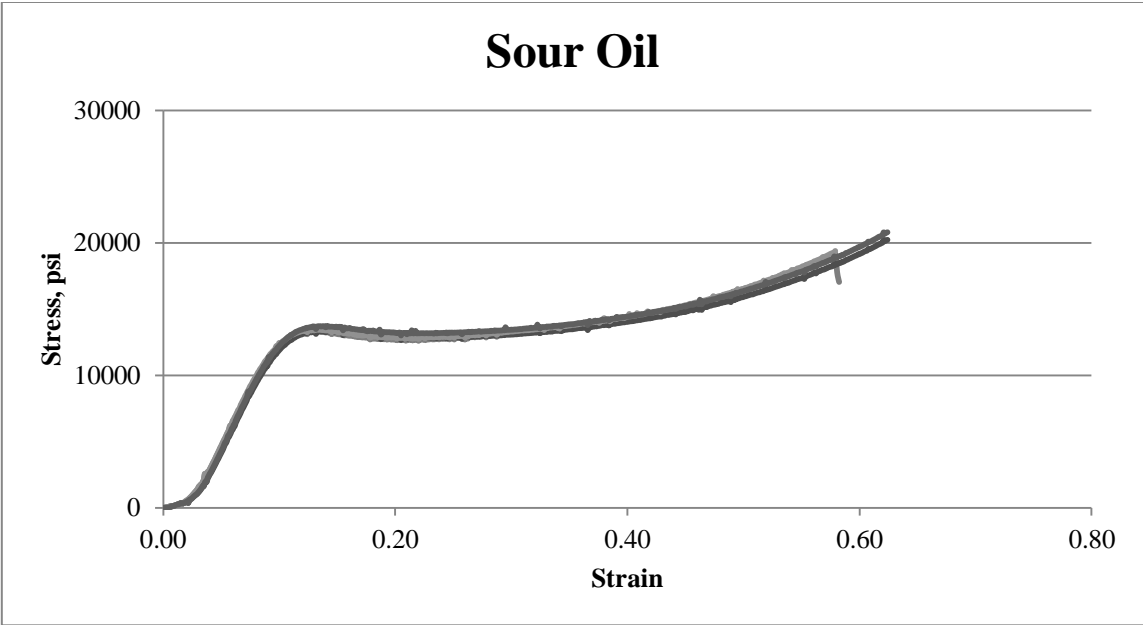


Fig. 46—The stress-strain curve from different experiment runs for epoxy-based resin with Sour Oil, tested under compression until failure



Fig. 47—A specimen of fully cured resin mixed with oil before and after the compression test

Fracture Strength

The compression test results displayed a clear reduction in the yield and ultimate compressive strengths of the resin, as a result of mixing with contaminants. While it is typical for ductile materials to fracture at the ultimate compressive strength, the pipe dope samples experienced fracture propagation at the yield strength. The constant stress after the yield point, or the slight increase in stress after the yield point, is the result of crack tolerance and the samples maintaining residual strength. The highest yield stress was that of pure resin at 13,940 psi, as shown in **Table 7**, followed by the pipe dope compositions of 2000, Metal-free, and OCTG with less than a 1% drop in yield strength each. The pipe dope composition of 4010NM and ZN18, and sour oil resulted in a 3% to 6% drop in yield strength. While API-modified and seawater caused the largest drop in yield strength of 10% to 11% or approximately 1,400 psi to 1,500 psi.

Table 7—AVERAGE YIELD STRENGTH		
	Average Yield Strength, psi	% Drop
Pure	13,940	0%
2000	13,920	0%
Metal free	13,810	1%
OCTG	13,810	1%
4010NM	13,510	3%
Oil	13,510	3%
ZN18	13,170	6%
API modified	12,520	10%
Seawater	12,470	11%

The majority of the samples tested had only one value that corresponded to both the yield strength and the fracture strength. Only two mixtures, other than pure resin,

maintained fracture strength greater than their yield strength. These mixtures were sour oil, and seawater, as shown in **Fig. 48**. The pure samples, oil samples, and seawater samples had yield strengths that were 58%, 63%, and 75% less than their ultimate strengths, respectively.

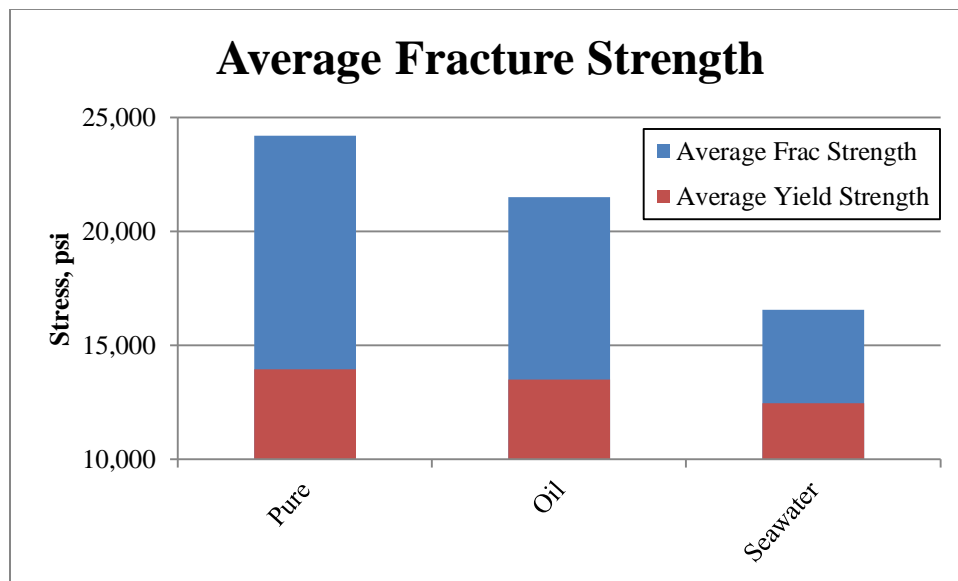


Fig. 48—The average fracture strengths of samples in comparison to their average yield strengths

The average fracture strengths of the oil and seawater samples were decreased by 11% and 32%, respectively, compared to pure resin. In comparison, the fracture strengths of the pipe dope mixtures resulted in a drop between 35% and 48% of the fracture strength of pure resin, as seen in **Table 8**.

Table 8—AVERAGE FRACTURE STRESS		
	Average Fracture Stress, psi	% Drop
Pure	24,190	0%
Oil	21,500	11%
Seawater	16,550	32%
2000	15,670	35%
Metal free	13,820	43%
OCTG	13,810	43%
4010NM	13,510	44%
ZN18	13,170	46%
API modified	12,520	48%

As shown in the results above, the addition of contaminants to pure epoxy resin reduced the maximum compressive strength and yield strength of the mixtures. The fracture strength corresponds to the maximum compressive strength for pure epoxy resin, the oil mixtures, and the seawater mixtures, but it corresponded to the yield strength for all pipe dope samples. The difference in fracture strengths between the samples tested was significantly greater than a 25% drop, while the yield strengths of all the samples remained relatively constant with the largest drop being as little as 11%.

CHAPTER V
EVALUATING THE EFFECT OF CONTAMINANTS ON THE CURE PROCESS
OF EPOXY RESIN

Objective

The application discussed in this thesis requires the resin to cure in the presence of wellbore chemicals. It is important to study the cure process of Epoxy Resin in the presence of seawater, oil, and pipe dope to understand the changes in terms of cure time and level of gelation relative to pure resin. During a 6 hour cure time, the criteria for defining a significant change from the cure process of pure resin, are a difference of 2 hours in the cure time or a reduced level of gelation of 4 at 6 hours.

Procedure

The experimental procedure to test the cure process included an oven to simulate the temperature in the wellbore. The resin was cured in 10-mL or 30-mL screw-cap glass vials, or 50-mL Ultra-High Performance Centrifuge Tubes. The experiments discussed in this chapter were performed following the steps described below:

1. Set the oven temperature to 200°F and allow it to reach steady state.
2. Prepare the first portion of the resin formulation by thoroughly mixing Part A resin and diluent in a beaker based on the ratios in Table 2 above.

3. Mix in Part B of the resin formulation based on the ratios in Table 2 above.
4. Fill the glass vials with seawater brine, sour oil, or pipe dope according to the proportions in **Table 9** to create 10, 20, 30, 40, and 50 wt % contaminant in resin mixtures.
5. Fill each of the 10-mL glass vials with resin for a total of 4.00 g of mixture.
6. Place the vials in the 200°F oven.
7. At 1 hour intervals, measure the level of gelation of the samples based on the qualitative test method in **Table 10** until they are fully cured.
8. Record the cure time for each sample.

	0 wt %	10 wt %	20 wt %	30 wt %	40 wt %	50 wt %
Mass of Resin, g	4.00	3.60	3.20	2.80	2.40	2.00
Mass of Contaminant, g	0.00	0.40	0.80	1.20	1.60	2.00

For each experiment cycle, 44 samples were prepared: five samples of 10, 20, 30, 40, and 50 wt % seawater brine, five samples of 10, 20, 30, 40, and 50 wt % Sour Oil, two samples for each of the 5 salts in seawater brine shown in Table 4, and 2 samples of 33 wt % of each of the 6 types of pipe dope shown in Table 3. In addition, for each run, at least two samples of resin without any contaminants were used with each test as the control. The samples were placed in the oven and analyzed at 1-hour intervals up to 7 hours. The experiments were repeated three times to confirm the results.

Level of Gelation

The level of gelation was determined qualitatively by a simple 0-5 qualitative test method. 0 indicates a resin with a water-like viscosity. 1 represents a resin with the same viscosity as the stable unreacted Part A fluid at room temperature. A level of gelation of 2 indicates a gel that moves or shakes when the vial is tilted or agitated. At a level of gelation of 3, the resin appears to be a solid but applying pressure on the surface when a 3-mm metal rod, shown in **Fig. 49**, easily penetrates the surface. At 4, the resin appears to be solid and applying pressure on the surface with a 3-mm metal rod creates a minor indentation but does not penetrate the surface. A level of gelation of 5 indicates a fully cured solid with no apparent indentation caused by pressure from the metal rod. The qualitative test method is listed in Table 10 below.



Fig. 49—The 3mm metal rod used in the qualitative level of gelation test

Table 10—THE LEVEL OF GELATION	
<u>Level of Gelation</u>	<u>Description</u>
0	Water-like viscosity
1	Thick liquid
2	Gel moves
3	Visually cured but applying pressure penetrates the surface
4	Cured but applying pressure creates minor indentation
5	Fully cured with no indentation when pressure is applied

Results and Discussion

Pure Epoxy-Based Resin

The pure epoxy-based resin was prepared following the procedure mentioned in the section above to form a clear orange colored viscous liquid, as shown in **Fig. 50**. The initial state of the resin was a thick liquid with a level of Gelation of 1. After the first hour in the 200°F oven, the viscosity of the resin decreased to a level of Gelation of 0.5. Hourly testing showed a gradual increase in the level of Gelation of the samples until full cure at 6 hours, as shown in **Fig. 51**.



Fig. 50—Thick, clear, orange colored, viscous epoxy resin

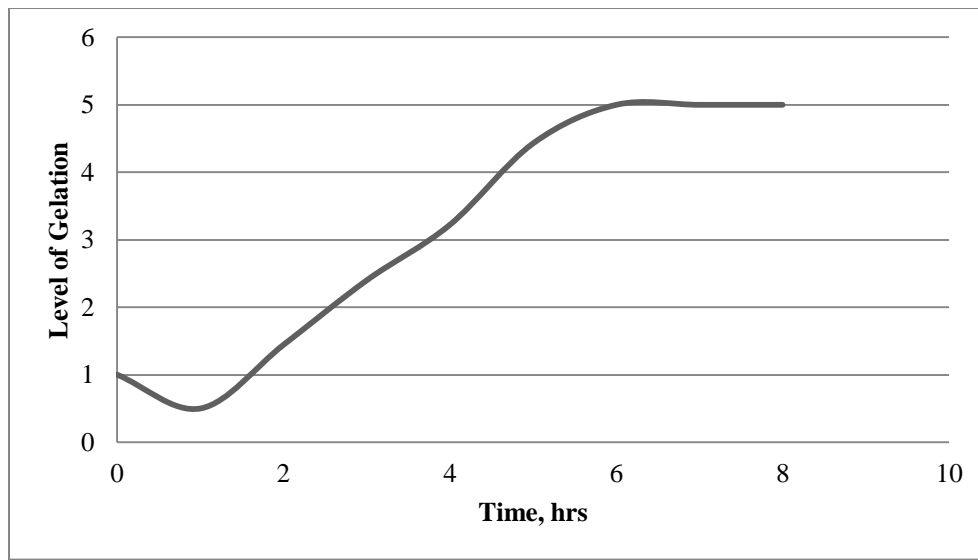


Fig. 51—The curing trend for pure epoxy-based resin which shows a decrease in the level of Gelation during the first hour, then a gradual increase until full cure at 6 hours

Seawater Brine

The presence of seawater brine in the mixture increased the rate of the cure process, starting from the first hour into the experiment. At 1 hour, the resin's viscosity had increased to a level of Gelation of 1.5, as opposed to the expected result of a decreased viscosity and 0.5 level of Gelation. The samples reached full cure in as little as 3 hours, compared to the 6 hours for pure resin. The results for the cure process tests of epoxy-based resin cured in the presence of seawater brine are shown in **Fig. 52**.

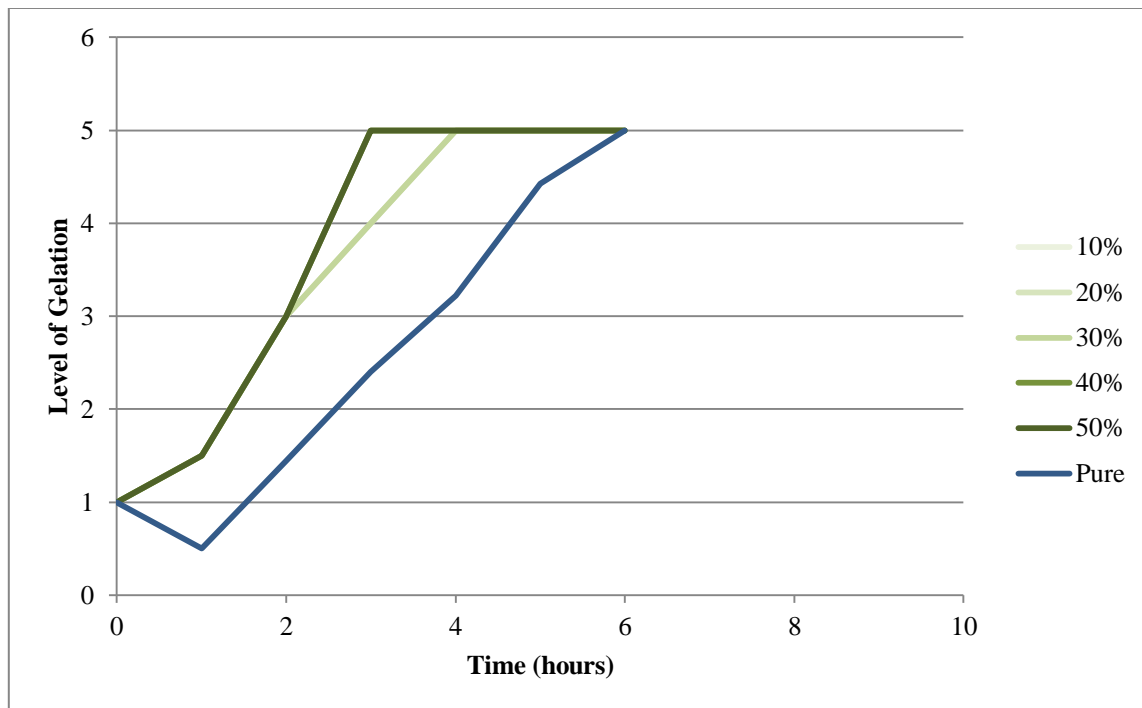


Fig. 52—The curing trend for epoxy-based resin in the presence of seawater brine at 10, 20, 30, 40, and 50 wt % seawater

Samples of each of the five salts of seawater brine were tested separately with epoxy-based resin to determine the effect of each salt. The resin was allowed to cure in the presence of ten different brines. Each salt brine was prepared with only one salt, and for each salt, two brines were prepared with a “High” and “Low” concentration as listed in **Table 11**.

Table 11—COMPOSITION AND CONCENTRATIONS OF 5 BRINES

<u>Salt</u>	<u>Name</u>	<u>Concentration, M</u>
<i>NaCl</i>	High	0.86
	Low	0.44
<i>CaCl₂·H₂O</i>	High	0.34
	Low	0.14
<i>MgCl₂·6H₂O</i>	High	0.25
	Low	0.14
<i>Na₂SO₄</i>	High	0.35
	Low	0.22
<i>NaHCO₃</i>	High	0.60
	Low	0.43

Each sample was mixed in a 1:1 (by weight) ratio of brine to resin, and the cure process was analyzed following the procedure above. The cure trend of the ten brines followed similar trends to that of seawater brine. The cure process was accelerated for all ten brines. All the high concentration brines were fully cured by 3 hours, similar to seawater brine but the high concentration mixtures with NaCl were fully cured in as little as 2 hours. For each salt solution, the high concentration mixtures showed accelerated curing trends than the corresponding low concentrations and a shorter cure period, as shown in **Fig. 53**.

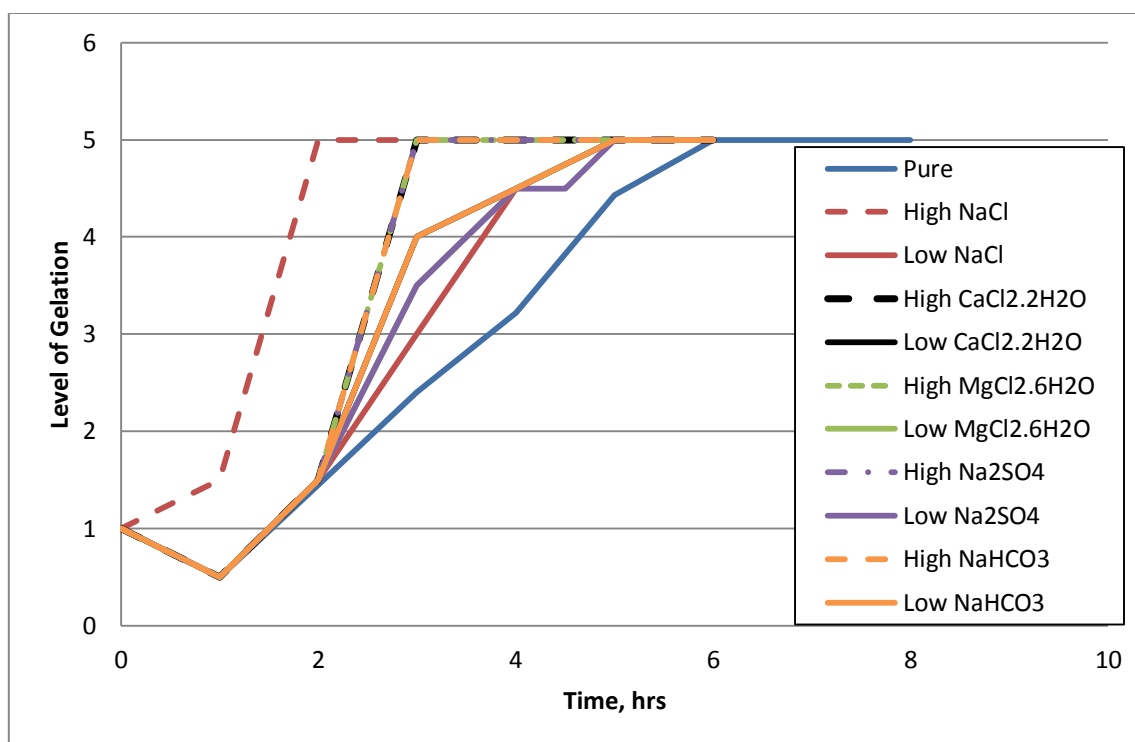


Fig. 53— The curing trend for epoxy-based resin in the presence of 50 wt % of 5 brines at 2 different concentrations

Sour Oil

For each test run, five different mixtures of epoxy-based resin with 10, 20, 30, 40, and 50 wt % sour oil were tested. The presence of sour oil in the mixtures did not significantly affect the rate of the cure process, compared to pure epoxy-based resin, as shown in **Fig. 54**. Several samples removed from the oven at 3 hours began showing effects of vitrification, as will be discussed in a later chapter. The phase change due to vitrification was recognized by the sudden rise in the level of Gelation as the sample cooled. This highlighted the importance of testing all the samples at the oven's 200°F to get more accurate bottomhole trends. The phase change with sour oil was accompanied

by a change in color of the mixtures from a clear black-brown color to an opaque light brown color as shown in **Fig. 55**.

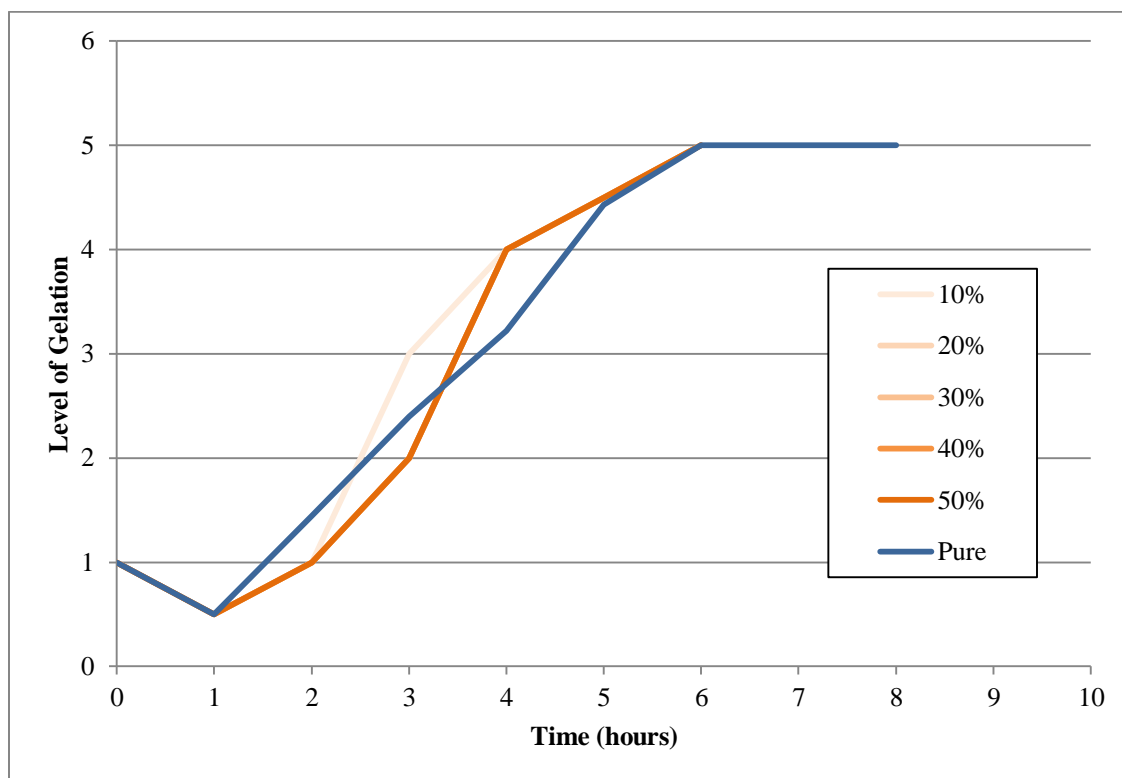


Fig. 54—The curing trend for epoxy-based resin in the presence of sour oil at 10, 20, 30, 40, and 50 wt % sour oil

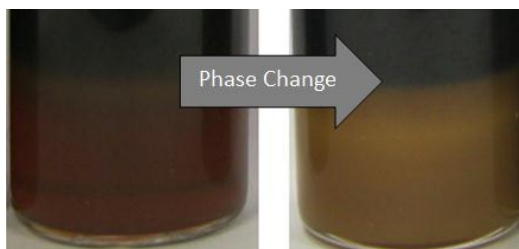


Fig. 55—The difference in color due to the phase change of resin mixed with sour-oil caused by the change in temperature from 200 °F to room temperature

Pipe Dope

Separate samples were prepared for each of the 6 types of pipe dope. Pipe dope is typically composed of organic grease and a mixture of inorganic materials. In these experiments, the samples all remained heterogeneous, where the inorganic material dropped out of solution and the organic material was mixed in with the resin. The samples exhibited altered curing trends. OCTG, 2000, and API-modified exhibited elastic properties at 4 hours, where applying pressure on the surface created an indentation but did not penetrate the surface. At 6.5 hours, these three mixtures maintained hard rubber properties. 4010NM, ZN18, and “Metal Free” remained at a level of Gelation below 3 up to 4 hours and “Metal Free” displayed an increased tackiness compared to pure resin. By 6.5 hours, the OCTG, 2000, API-modified, ZN18, and “Metal Free” maintained a hard rubber texture, but had not fully cured. 4010NM, on the other hand, had separated at 4 hours into 3 phases. The topmost phase was a water-like liquid, a low viscosity resin in the middle, and the inorganic material at the bottom. At 5 hours it remained very soft and tacky with a level of Gelation of 3, then at 6.5 it became a soft elastic material with a level of Gelation less than 4, as shown in **Fig. 56**. In less than 24 hours all samples had fully cured, but maintained heterogeneity in the mixture which affected the mechanical strength of the sample.

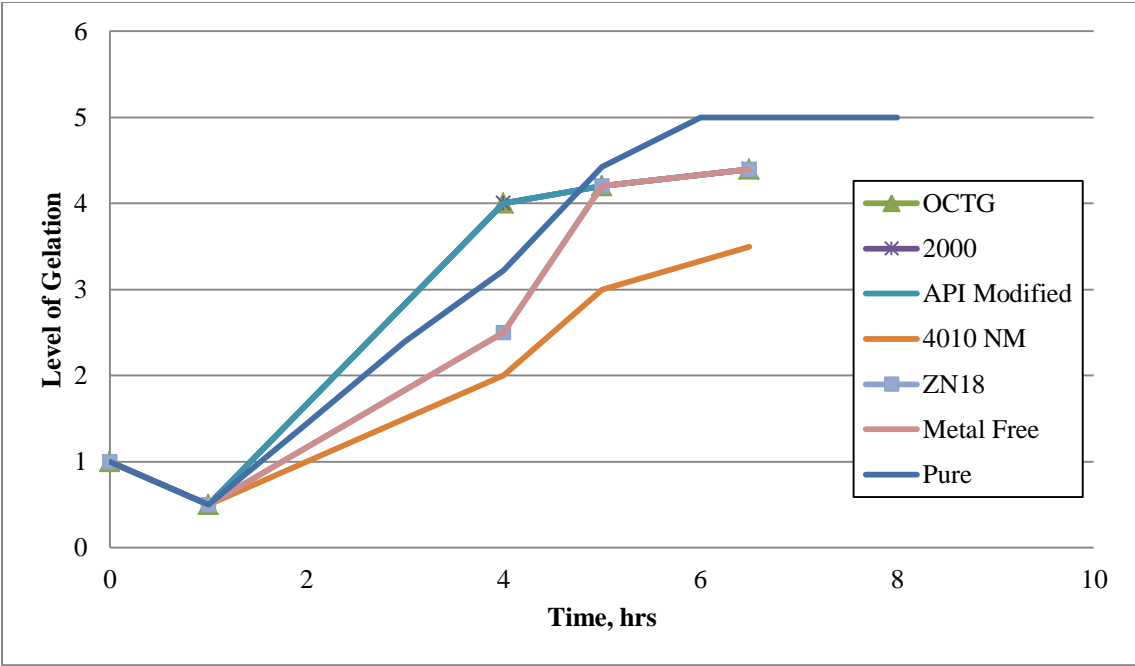


Fig. 56—The curing trend for epoxy-based resin in the presence of the 6 types of Best-o-life pipe dopes: OCTG, 2000, API modified, 4010NM, ZN18, and Metal Free

CHAPTER VI
EVALUATING THE USE OF SOLID EPOXY RESIN BEADS AS A
PLACEMENT METHOD

Background

Vitrification and Gelation

A time-temperature-transformation (TTT) isothermal cure diagram, shown in **Fig. 57**, can be used for understanding the cure properties of thermosetting systems (Dawkins 1986; Gillham 1985). The main events of such a diagram include the onset of gelation, vitrification, and full-cure. Gelation corresponds to the formation of an infinite molecular network, according to Flory's theory of gelation (Flory 1953). Vitrification, a completely distinct phenomenon from gelation, can occur at any stage during the reaction to form either an ungelled glass or a gelled glass. In the glassy state, the rate of reaction undergoes a significant decrease but is not zero. Unlike gelation, vitrification is reversible by heating, and the cure process may be reestablished by heating to devitrify the partially cured Epoxy (Menczel 2009).

During the cure process, the system follows the isothermal line labeled as “Cure Process” in **Fig. 57** where the resin goes through gelation, vitrification, and eventually full cure. Interrupting the cure process at a time, t , by reducing the temperature of the resin, will cause the resin to vitrify into an ungelled glass and significantly decrease the reaction rate. The time at the point of gelation is assumed to be the cure time, then, according to **Fig. 57**, the point of vitrification at T_{gel} is greater than the cure time.

Portland Cement

Standard procedures in the oil and gas industry involve using Portland cement, ASTM types I and II, as the plugging material. ASTM standards define the properties of these cement mixtures; ten such mixtures are defined in ASTM C150/C150M with compressive strengths included and listed in **Table 12** below (ASTM 2009). The compressive strength values defined in ASTM C150/C150M are based on uniaxial compressive tests performed on 2-in cement cube specimens as defined in ASTM C109/C109M (ASTM 1999b). Cube specimens are always stronger than cylinders due to cubes having an overlapped restrained zone towards the corners while testing under uniaxial compression, hence, a zone of triaxial compression develops.

Table 12—PORTLAND CEMENT COMPRESSIVE STRENGTHS(Data from ASTM C150/C150M)

<u>Cement Type</u>	<u>Compressive Strength, psi</u>
I	4080
IA	4080
II	3190
IIA	3190
II(MH)	4060
II(MH)A	3190
III	3480
IIIA	2760
IV	2470
V	3050

Objectives

1. Determine whether the vitrification point of epoxy resins successfully allows the formation of solid beads without gelation. Secondly, determine whether the vitrified solid beads can be stored for a period of time greater than double the 6-hour cure period of the resin. Finally, determine whether the solid beads can be devitrified at wellbore temperature and reconsolidate into one mass and cure.
2. Determine if the compressive strength of the reconsolidated resin solid can be an improvement over Portland cement, specifically creating an increase in strength of up to 50%.
3. Analyze the operational cost savings by comparing the use of vitrified resin beads to conventional cement. Determine cost savings created by reducing the material losses due to using vitrified epoxy resin beads in place of pumping liquid epoxy in a 7,000-ft application.

Procedure

The parts of epoxy-based resin were mixed and allowed to partially cure in an oven. Before gelation occurs at high temperature, the resin was removed and solid beads were formed by cooling the fluid. The resin was stored then returned to the oven to

continue the curing process. The resin was prepared following the steps mentioned below:

1. Set the oven temperature to 200°F and allow it to reach steady state.
2. Prepare the first portion of the resin formulation by thoroughly mixing the Part A resin and diluent in a beaker based on the ratios in Table 2 above.
3. Mix in Part B of the resin formulation based on the ratios in Table 2 above.
4. Mix in 50% (by weight) of oil.

To be able to create vitrified solid resin beads at any time, t , the fluid should be in liquid form at 200°F and in solid form at 39°F, at the same time t . At 200°F, the resin must maintain a low enough viscosity to be transported with a syringe. While at 39°F, the solid beads must be capable of maintaining their shape and must not exhibit a tacky surface that adheres to surfaces or other beads. To test these two conditions requires the use of two qualitative test methods that will be described below. The following list describes the steps required to find time t at which solid beads can be formed:

5. Separate the resin-oil mixture into two equal batches, called Batch A and Batch B
6. Divide each batch into 5-mL samples over eight 10-mL glass vials.
7. Place all 16 glass vials upright in the oven at 200°F
8. At 1-hour intervals

- a. Remove 1 glass vial from Batch A from the oven and allow it to cool to room temperature. Ensure the glass vial remains upright.
 - b. Turn 1 glass vial from Batch B onto its side so it is lying horizontally in the 200°F oven.
9. After 12 hours from the initiation of the experiment
- a. Measure the level of Gelation of Batch A samples based on the qualitative test method of Table 10.
 - b. Classify Batch B samples based on the Sydanski qualitative test method listed in **Table 13**
10. Determine time, t , at which the resin formulation in question can be transformed from a liquid to a solid by a sudden drop in temperature from 200°F to 39°F.

Table 13—GEL STRENGTH CODE (Sydanski 1989)

A	No detectable gel formed: the bulk of the system has the same viscosity as the polymer solution
B	High flow gel: slightly more viscous than the polymer solution
C	Flowing gel: most of the gel flows to the bottle cap upon inversion
D	Moderately flowing gel: only a portion of the gel (~5-10%) does not flow to the bottle cap
E	Barely flowing gel: gel can barely flow to the bottle cap and/or a significant portion (>15%) does not flow to the cap
F	Highly deformable nonflowing gel: gel does not flow to the cap
G	Moderately deformable nonflowing gel: gel deforms about half way down the bottle upon inversion
H	Slightly deformable nonflowing gel: only the gel surface slightly deforms upon inversion
I	Rigid gel: no gel surface formation by gravity upon inversion
J	Ringing rigid gel: a tuning fork-like mechanical vibration can be felt upon tapping the bottle

The Sydansk test method is used to examine Batch B samples once the experiment is over. The purpose of turning the vials on their side is to allow any liquid resin to flow along the walls of the vial. By keeping the vials in the oven, it ensures that the amount of resin that flowed along the walls will cure and allow the examiner to determine the gel strength code of that specimen. An uncured sample will have the bulk of the resin along the wall of the vial up to the lid, while a cured sample will have the bulk of the resin at the base of the vial with no lip on the wall.

The resin mixture at 200°F continues to cure, as long as the temperature of the mixture remains at 200°F. Solid beads can be formed by allowing the resin to cool to room temperature, but quenching the mixture in 39 °F water allows a faster solidification and ensures the curing process has been suspended. The following steps describe the process of forming the solid beads:

11. Repeat steps 1 to 4
12. Place the mixture in the 200°F oven until time t .
13. Use a syringe to inject droplets of the resin mixture into 39°F water to quench the resin and form solid beads.
14. Store the solid beads at 39°F to maintain long shelf life

When the solid beads are needed to be tested, they can be placed at 200°F, where they liquefy then continue the cure process to form one solid mass. It is important to note that the cure process does not stop completely during storage; it is simply slowed down significantly.

15. Place solid beads in 50-mL Ultra-High Performance Centrifuge Tubes and place them in the 200°F oven until the beads have liquefied then fully cured.
16. Removed the cured samples from the 50-mL Ultra-High Performance Centrifuge Tubes.

It is important for uniaxial compression tests to maintain a load vector parallel to the axis of the sample being tested. As a result, the samples are required to have ends that are parallel to each other and the surfaces of the compression machine. The ends are also required to be square with the sides of the cylinder to ensure uniform loading and deformation. The following list describes the steps necessary to achieve these requirements:

1. Remove the cured solid samples from the 50-mL Ultra-High Performance Centrifuge Tubes.
2. Use a band-saw to cut off the conical end of the sample and to cut the samples into two 1-inch long cylinders.
3. Sand the ends of the samples on a disc sander to ensure parallel ends to the sample as well as to smooth off the surface for an adequate compression test surface.
4. Measure the height and average diameter of each specimen.

5. Check each sample for its conformance to the requirement of parallel top and bottom ends. Any sample that does not meet the specifications is unsuitable for testing.

The compression tests were run using an Instron 4206 connected to a computer running a Labview data acquisition program. For each run, the machine was allowed to apply a load on the sample, until the sample failed or the load reached the load limit of 30,000 psi. A sample failing is indicated by a sudden drop in the measured load. The following steps list the directions used to run the compression tests and collect the data points:

6. Turn on the Instron 4206.
7. On the control panel hit "Load Cal" then "Enter"
8. Hit "Load Bal" then "Enter"
9. Hit "GL reset"
10. Hit "Speed" and set it to 0.2 inches per minute.
11. Launch the Labview program.
12. Start data acquisition by running the Labview program.
13. Hit the "Down" button to start the Instron.
14. Stop the machine when the sample fails or reaches the load limit of 30,000 psi.

Results and Discussion

The Batch B samples were turned on their side every hour, as mentioned above and kept in the oven. Once the time of the experiment was completed the samples were removed and examined. The samples from the first 4 hours, in **Fig. 58**, show the resin flowed to the lid of the vials while the vials were horizontal. The black fluid at the base of the vials in the images of this section, is the residual oil portion of the mixture, while the brown fluid/solid is the thermosetting portion of the mixture.

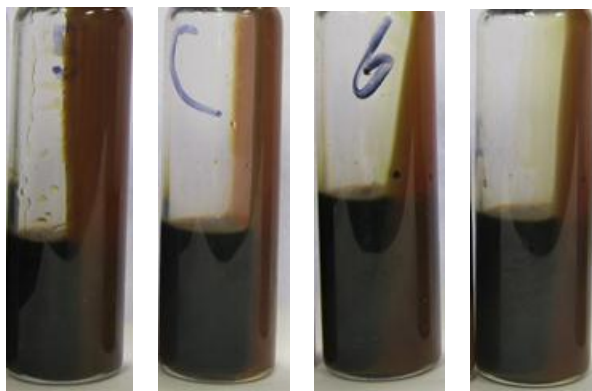


Fig. 58—The 1-hour, 2-hour, 3-hour, and 4-hour samples of Batch B repositioned and kept in the 200°F oven

At the 5-hour sample, signs of gelation began to appear. The majority of the resin remained at the base of the vial, but a portion created a lip halfway up to the lid of the vial, as seen in **Fig. 59**.

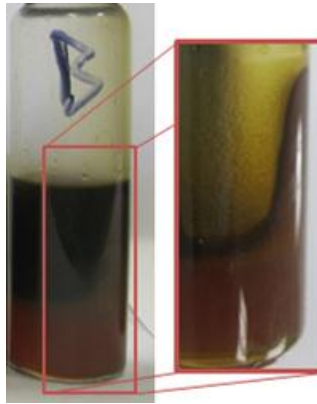


Fig. 59—The 5-hour samples of Batch B repositioned and kept in the 200°F oven

The 6-hour, 7-hour, and 8-hour samples showed no movement in the resin, as seen in **Fig. 60**, indicating that the resin at this point will maintain its shape until fully cured.

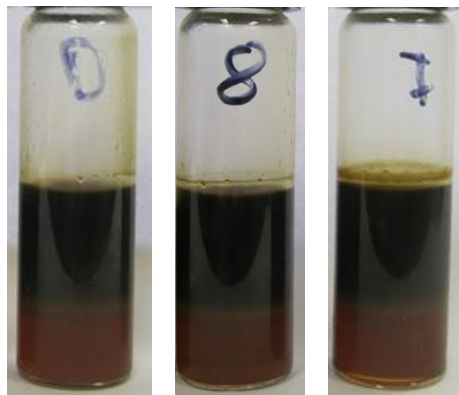


Fig. 60—The 6-hour, 7-hour, and 8-hour samples of Batch B repositioned and kept in the 200°F oven

One sample from Batch A was removed from the oven every 1 hour, and allowed to cool to room temperature. Each sample was tested using the qualitative test in Table

10 after the first 12 hours had passed. The results displayed a progressively hardening trend, starting from the 2-hour sample at a level of gelation of 1, to the 6-hour sample at a level of gelation of 5. **Fig. 61** shows the hardening trend of Batch A compared to the results from Batch B. It is apparent that Batch B at 200°F, had a 2-hour delay in the onset of gelation compared to Batch A. At 4 hours, Batch B samples remained a flowing liquid while Batch A had a level of Gelation of 3, corresponding to a resin that is visually cured but applying pressure penetrates the surface. Therefore, to create the vitrified solid resin beads the time, t , at which the cure process should be stopped, is 4 hours.

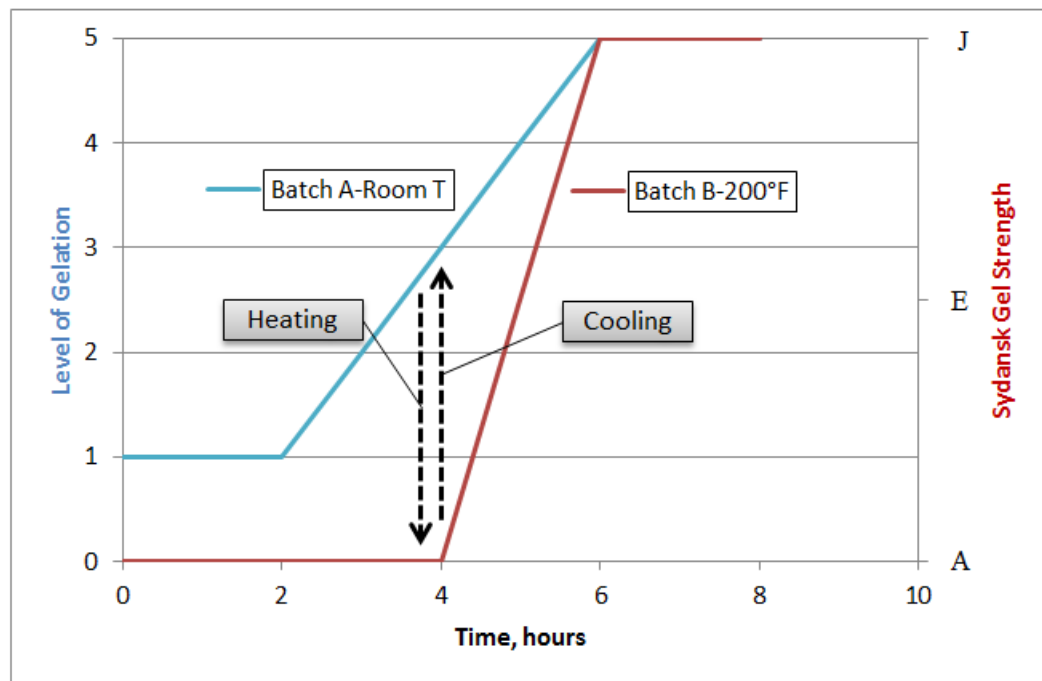


Fig. 61—The trends of Batch A and Batch B samples showing the effect of temperature on gel strength

At 3.5 to 4 hours the resin can be removed from the oven at 200°F and cooled down rapidly to 39°F to instantly form solids, shown in **Fig. 62**. This was done using a syringe to remove the resin from the vial and place it, as droplets, in ice water. Once the droplets were solidified they would then be placed in a beaker and put in a refrigerator.



Fig. 62—Vitrified resin droplets that were formed by quenching droplets of resin in 39°F water 3.5 hours into the cure process

Once the beads are needed, they can be placed back in the oven. The vitrified resin beads began devitrification at approximately 130°F. Once in liquid form, the material reconsolidated and continued the cure process in the 50-mL Ultra-High Performance Centrifuge Tubes until fully cured. The resin mixture cured to one consolidated solid, but bubbles were observed in the material, as seen in **Fig. 63**, due mainly to the fact that when the beads liquefy, the viscosity is greater than that of the pure liquid epoxy resin, resulting in slower bubble release and heterogeneity in the final solid.

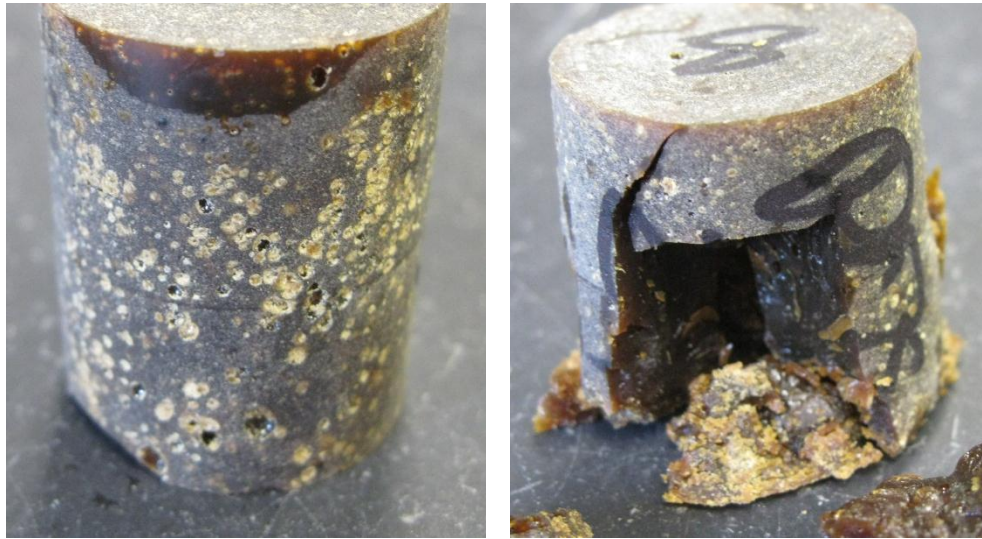


Fig. 63—A specimen of fully-cured reconsolidated epoxy-resin beads before and after the compression test

The cured solid was removed from the centrifuge tubes, machined, and sanded in preparation for a compression test. The stress-strain curve produced from the compression tests are shown in **Fig. 64**. As the load increases beyond the yield point, pore collapse causes the strain to increase until, eventually, the specimen fractures and fails completely. The fracture strength, in this case, has the same value as the yield strength of the specimens. These samples did not exhibit any barreling; instead they deformed axially then broke into several pieces. The average fracture strength was found to be 7,717 psi, which is 89% more than the compressive strength value of Portland cements I & II in Table 12, but also corresponds to a 45% drop from the yield strength of pure resin. The heterogeneity in the solid is the largest contributor to the drop in fracture strength, due to the bubbles aiding in crack initiation and propagation.

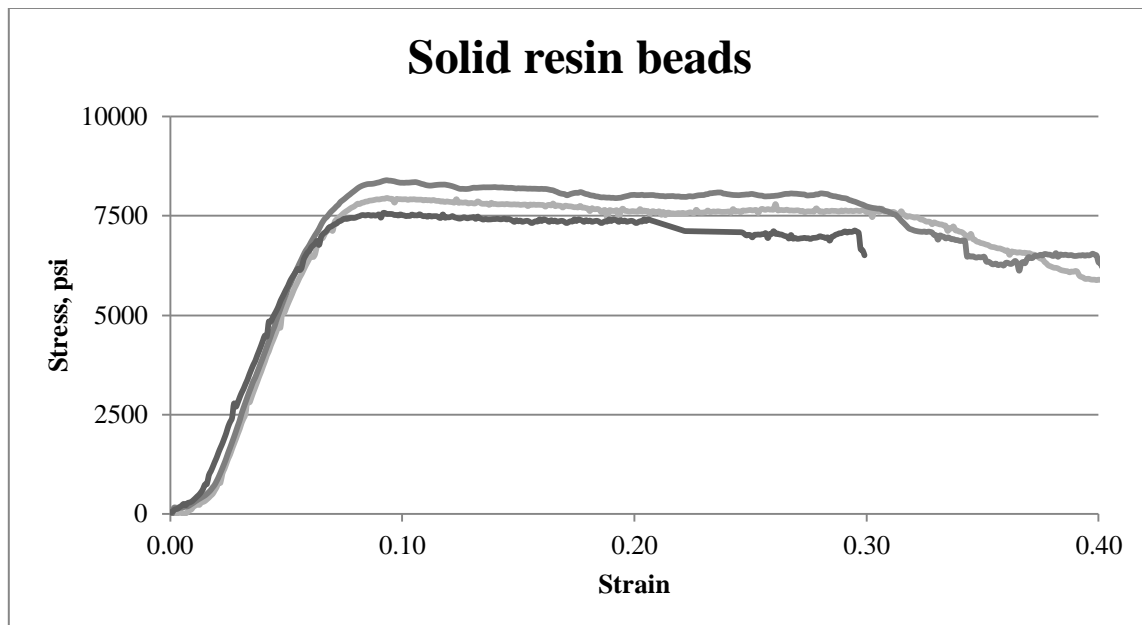


Fig. 64—The stress-strain curve for reconsolidated epoxy resin beads tested under compression until failure

Cost Analysis

A cost comparison between two P&A operations was performed to determine the cost benefits to using vitrified solid resin beads over conventional Portland cement. In the first case, with the resin beads, an offset well was drilled to a depth of 1,000-ft below the mudline, where the beads were pumped and allowed to drop in the annulus and settle for 6,000 ft to the top of the packer. The second case, with Portland cement, the offset well was drilled 7,000 ft below the mudline, and cement was spotted in place. The cost comparison for the two cases is shown in **Table 14**.

Table 14—COST COMPARISON FOR P&A

	<u>Resin Beads</u>	<u>Portland Cement</u>
Material Cost	\$190,000 ^a	\$23,800 ^b
Drilling Cost	\$143,700 ^c	\$1,005,800 ^d
Total	\$333,700	\$1,029,600

a) Approximated based on the cost of UltraSeal at \$10,000/bbl and a plug height of 550 ft in 6-in tubing
b) Approximated based on the cost of Portland Cement at \$1,250/bbl and a plug height of 550 ft in 6-in tubing
c) Approximate drilling cost for 1,000-ft at a rate of 116 ft/min and a \$400,000/day equipment cost (Kaiser M.J 2008)
d) Approximate drilling cost for 7,000-ft at a rate of 116 ft/min and a \$400,000/day equipment cost (Kaiser M.J 2008)

While the cost of UltraSeal is approximately 8 times the cost of Portland cement, the time required to drill the offset well and apply the resin beads is significantly reduced, and subsequently the cost is reduced. There is a potential for USD 0.7 million in savings using this system, based on the assumptions made in this section. In addition, using resin beads reduces the amount of material loss on the walls of the well. According to El-Mallawany, up to 32% of material can potentially adhere to the casing and not settle on the packer (El-Mallawany 2011). 32% of the cost of epoxy required for the application is approximately USD 60 thousand for a 7,000-ft application with a 550-ft plug height.

CHAPTER VII

CONCLUSIONS

1. Mixing the resin with seawater, oil, or pipe dope will reduce the ultimate strength and fracture strengths of the mixtures compared to the strengths of pure resin. The ultimate strength of contaminated resin will most likely drop to the value of the yield strength, and should be designed with that in mind. The fracture strengths of contaminated resin will experience a drop greater than a 25% compared to pure resin, while the yield strength, on the other hand, can remain relatively unaltered.
2. During a 6-hour cure, the cure process of resin mixed in with seawater can be accelerated by more than 2 hours compared to pure resin, while oil has no apparent effect on the cure process.
3. Quenching droplets of epoxy resin in 39°F diluted water before the initiation of gelation during the cure process was found to form solid beads through the reversible physical process of vitrification; using this effect as a plugging application can be successful.
4. The average fracture strength of reconsolidated epoxy resin beads was found to be 7,717 psi, indicating that an application utilizing solid resin beads, as discussed in this thesis, can be up to 89% stronger than the ASTM compressive strength values for Portland cements I & II.

5. From an operational cost standpoint, using vitrified epoxy resin beads has the potential to create up to USD 0.7 million in savings compared to conventional cement costs for cases similar to the one discussed herein. In Addition, using vitrified epoxy resin beads in place of pumping liquid epoxy resin could eliminate the 32% of material lost during settling, thus creating savings of approximately USD 60 thousand for a 7,000-ft application with a 550-ft plug height.

REFERENCES

- API. 1999. Temperatures for API Cement Operating Thickening Time Tests. In. Washington DC: American Petroleum Institute. 10TR3
- ASTM. 1999a. C42/C42m Test Method for Obtaining and Testing Drilled Cores and Sawed Beams of Concrete. In. West Conshohocken, PA: ASTM International.
- ASTM. 1999b. C109/C109m Test Method for Compressive Strength of Hydraulic Mortars. In. West Conshohocken, PA: ASTM International.
- ASTM. 2009. C150/C150m Specification for Portland Cement. In. West Conshohocken, PA: ASTM International.
- Barclay, I.S., Johnson, C.R., Staal, T.W., Choudhary, S., and Al-Hamandani, A. Utilizing Innovative Flexible Sealant Technology in Rigless Plug and Abandonment. Paper presented at the *SPE/ICoTA Coiled Tubing Conference and Exhibition*, Houston, TX. March 2004. 89622. DOI: 10.2118/89622-ms
- BOEMRE. 2011. *Gulf of Mexico OCS Oil and Gas Lease Sale: 2011*. New Orleans, LA: U.S. Department of the Interior.
- Calvert, D.G. and Smith, D.K. Issues and Techniques of Plugging and Abandonment of Oil and Gas Wells. Paper presented at the *SPE Annual Technical Conference and Exhibition*, New Orleans, LA. September 1994. 28349. DOI: 10.2118/28349-ms
- Case, J., Chilver, L., and Ross, C.T.F. 1999. *Strength of Materials and Structures*. Burlington, MA: Butterworth-Heinemann.
- Chong, K.K., Charles A. Butterfield, J., and Conwell, R.P. Novel Technique for Openhole Abandonment Saves Rig Time-a Case History. Paper presented at the *SPE Asia Pacific Oil and Gas Conference and Exhibition*, Brisbane, Australia. October 2000. 64481. DOI: 10.2118/64481-ms
- Dawkins, J.V. 1986. *Developments in Polymer Characterisation*. New York: Elsevier Applied Science Publishers.
- El-Mallawany, I.I. 2011. An Experimental Setup to Study the Settling Behavior of Epoxy Based Fluids. Masters of Science, Texas A&M University, College Station, TX.
- Flory, P.J. 1953. *Principles of Polymer Chemistry*. Ithaca, NY: Cornell University Press.

- Gillham, J.K. 1985. Cure and Properties of Thermosetting Systems. *British Polymer Journal* **17** (2): Pp. 224-226. DOI: 10.1002/pi.4980170225
- Gougler Jr., P.D., Hendrick, J.E., and Coulter, A.W. Field Investigation Identifies Source and Magnitude of Iron Problems. Paper presented at the *SPE Production Operations Symposium*, Oklahoma City, OK. January 1985. 13812. DOI: 10.2118/13812-ms
- Holub, R.W., Noel, R.P., and Weinbrandt, R.M. Scanning Electron Microscope Pictures of Reservoir Rocks Reveal Ways to Increase Oil Production. Paper presented at the *SPE Symposium on Formation Damage Control*, New Orleans, LA. January 1974. 4787. DOI: 10.2118/4787-ms
- Irfan, M.H. 1998. *Chemistry and Technology of Thermosetting Polymers in Construction Applications*. New York; Dordrecht, Netherlands: Springer - Verlag.
- Kabir, A.H. Chemical Water & Gas Shutoff Technology - an Overview. Paper presented at the *SPE Asia Pacific Improved Oil Recovery Conference*, Kuala Lumpur, Malaysia. October 2001. 72119. DOI: 10.2118/72119-ms
- Kelland, M.A. 2009. *Production Chemicals for the Oil and Gas Industry*. Boca Raton, FL: CRC Press.
- Kelm, C.H. and Faul, R.R. Well Abandonment- a "Best Practices" Approach Can Reduce Environmental Risk. Paper presented at the *SPE Asia Pacific Oil and Gas Conference and Exhibition*, Jakarta, Indonesia. April 1999. 54344. DOI: 10.2118/54344-ms
- Loewen, K., Chan, K.S., Fraser, M., and Leuty, B. A Well Stimulation Acid Tube Clean Methodology. Paper presented at the *Annual Technical Meeting*, Calgary, Alberta. January 1990. 90-47. DOI: 10.2118/90-47
- Maly, G.P. Close Attention to the Smallest Job Details Vital for Minimizing Formation Damage. Paper presented at the *SPE Symposium on Formation Damage Control*, Houston, Texas. January 1976. 5702. DOI: 10.2118/5702-ms
- Mcleod Jr., H.O. 1984. Matrix Acidizing. *SPE Journal of Petroleum Technology* (12). DOI: 10.2118/13752-pa
- Mcleod Jr., H.O., Ledlow, L.B., and Till, M.V. The Planning, Execution, and Evaluation of Acid Treatments in Sandstone Formations. Paper presented at the *SPE Annual Technical Conference and Exhibition*, San Francisco, CA. January 1983. 11931. DOI: 10.2118/11931-ms

- Menczel, J.D., Prime, R. Bruce. 2009. *Thermal Analysis of Polymers: Fundamentals and Applications*. Trans Menczel, J.D., Prime, R. Bruce. Hoboken, NJ: John Wiley & Sons.
- Nasr-El-Din, H.A., Al-Mutairi, S.H., and Al-Driweesh, S.M. Lessons Learned from Acid Pickle Treatments of Deep/Sour Gas Wells. Paper presented at the *International Symposium and Exhibition on Formation Damage Control*, Lafayette, LA. February 2002. 73706. DOI: 0.2118/73706-ms
- Ng, R.C. 1995. *Low Temperature Epoxy System for through Tubing Squeeze in Profile Modification, Remedial Cementing, and Casing Repair*. Doc. 5,377,757, pt. United States: Mobil Oil Corporation.
- P.F.S. 2007. Liquid Bridge Plug/ Ultra Seal R Micro Annular Gas Migration Shut Off. In: Professional Fluids Services, LLC.
- Peng, W. and Riedl, B. 1995. Thermosetting Resins. *Journal of Chemical Education* **72** (7): 587. DOI: 10.1021/ed072p587
- Sydansk, R.D. 1989. *Delayed in Situ Crosslinking of Acrylamide Polymers for Oil Recovery Applications in High-Temperature Formations*. Doc. US 4844168, pt.
- Tettero, F., Barclay, I., and Staal, T. Optimizing Integrated Rigless Plug and Abandonment - a 60 Well Case Study. Paper presented at the *SPE/ICoTA Coiled Tubing Conference and Exhibition*, Houston, TX. March 2004. 89636. DOI: 10.2118/89636-ms
- Wei, R.P. 2010. *Fracture Mechanics - Integration of Mechanics, Materials Science, and Chemistry*. New York: Cambridge University Press.

VITA

Name: Ahmed Rami Abuelaish

Address: Harold Vance Department of Petroleum Engineering
Texas A&M University
3116 TAMU - 507 Richardson Building
College Station, TX 77843-3116

Email Address: ahmed.abuelaish@pe.tamu.edu

Education: B.S., Mechanical Engineering, Texas A&M University, 2009
M.S., Petroleum Engineering, Texas A&M University, 2011